

**Journal of
Pharmacognosy and
Phytotherapy**

Volume 8 Number 5, May 2016
ISSN 2141-2502



*Academic
Journals*

ABOUT JPP

The **Journal of Pharmacognosy and Phytotherapy (JPP)** is published monthly (one volume per year) by Academic Journals.

The **Journal of Pharmacognosy and Phytotherapy (JPP)** is an open access journal that provides rapid publication (monthly) of articles in all areas of the subject such as ethnobotany, phytochemistry, ethnopharmacology, zoopharmacognosy, medical anthropology etc.

The Journal welcomes the submission of manuscripts that meet the general criteria of significance and scientific excellence. Papers will be published shortly after acceptance. All articles published in JPP are peer-reviewed.

Contact Us

Editorial Office: jpp@academicjournals.org

Help Desk: helpdesk@academicjournals.org

Website: <http://www.academicjournals.org/journal/JPP>

Submit manuscript online <http://ms.academicjournals.me/>

Editors

Dr. (Mrs) Banasri Hazra

Research Scientist (U.G.C.)
Department of Pharmaceutical Technology
Jadavpur University
Calcutta - 700032
India

Dr. Yuanxiong Deng

Dept of Pharmaceutical Science
School of Medicine
Hunan Normal University
Tongzipo Road 371, Changsha 410013,
Hunan China

Prof. Maha Aboul Ela

Beirut Arab University, Faculty of Pharmacy, Beirut
Campus

Dr. S. RAJESWARA REDDY

Assistant Professor, Division of Animal Biotechnology
Department of Biotechnology, School of Herbal
Studies and Naturo Sciences,
Dravidian University, Kuppam – 517 425, A.P.
India

Dr. Mekhfi Hassane

University Mohammed the First, Faculty of Sciences,
Department of biology, Oujda, Morocco
Morocco

Dr. Ilkay Erdogan Orhan

Faculty of Pharmacy, Gazi University,
Ankara, Turkey
Turkey

Dr. Arun Kumar Tripathi

Central Institute of Medicinal and Aromatic Plants
P.O. CIMAP, LUCKNOW-226015,
India

Dr. Wesley Lyeverton Correia Ribeiro

Universidade Estadual do Ceará, Faculdade
de Veterinária/Laboratório de Doenças
Parasitárias Av. Paranjana, 1700
Itaperi - Fortaleza
60740-903, CE - Brazil

Dr. Maryam Sarwat

C/O A.M. Khan, House No. 195

Dr. Yong-Jiang Xu

Saw Swee Hock School of Public Health,
National University of Singapore, Singapore.

Prof. Dr. Adeolu Alex Adedapo

Department of Veterinary Physiology,
Biochemistry and Pharmacology
University of Ibadan, Nigeria

Dr. Joana S. Amaral

Campus de Sta Apolónia,
Ap. 1134, 5301-857 Bragança,
Portugal

Dr. Asad Ullah Khan

Interdisciplinary Biotechnology UNIT
Aligarh Muslim University,
India

Dr. Sunday Ene-ojo Atawodi

Biochemistry Department
Ahmadu Bello University
Zaria, Nigeria

Prof. Fukai Bao

Department of Microbiology and Immunology,
Kunming Medical College
China

Dr. Bhaskar C Behera

Agharkar Research Institute
Dept. of Science & Technology,
Plant Science Division
India

Prof. R. Balakrishna Bhat

Walter Sisulu University
Department of Botany
Mthatha, South Africa

Dr. Mohammad Nazrul Islam Bhuiyan

BCSIR Laboratories;
Chittagong cantonment;
Chittagong-4220;
Bangladesh

Dr. Baojun Bruce Xu

Beijing Normal University-Hong Kong Baptist
University United International College Zhuhai,
Guangdong Province,
China

Dr. Hamad H. Issa

Department of Physical Sciences,
School of natural Sciences,
The University of Dodoma,
Tanzania

Dr. Gagan Deep

Department of Pharmaceutical Sciences
School of Pharmacy,
University of Colorado Denver,
Colorado,
USA

Dr. Fengguo Xu

Dept of Epidemiology and Public Health,
Yong Loo Lin School of Medicine,
National University of Singapore,
Singapore

Dr. Haitao Lv

Medicine and Endocrinology,
Albert Einstein College of Medicine,
Yeshiva University,
USA

Hassane MEKHF

University Mohammed the First,
Faculty of Sciences,
Department of biology,
Laboratory of Physiology and Ethnopharmacology,
Morocco

Dr. Subhash C. Mandal

Division of Pharmacognosy
Pharmacognosy and Phytotherapy Research
Laboratory,
Department of Pharmaceutical Technology,
Jadavpur University,
India.

Dr. Adibe Maxwell Ogochukwu

Clinical Pharmacy and Pharmacy Management,
Faculty of Pharmaceutical Sciences,
University of Nigeria, Nsukka
Enugu state,
Nigeria.

Dr. Odukoya, Olukemi Abiodun

Department of Pharmacognosy,
Faculty of Pharmacy
University of Lagos.
Nigeria.

Dr. Qinxue Richard Ding

Medical Center at Stanford University,
Palo Alto,
USA

Dr. Sulejman Redžić

Faculty of Science of the University of Sarajevo
33-35 Zmaja od Bosne St.,
Sarajevo,
Bosnia and Herzegovina

Dr. Michal Tomczyk

Medical University of Bialystok,
Faculty of Pharmacy,
Department of Pharmacognosy,
Poland

Dr. Ugur Çakilcioglu

Firat University,
Faculty of Science and Arts,
Department of Biology,
Elazig
Turkey

Prof. Samson Sibanda

National University of Science and Technology
Cnr Gwanda Road/Cecil Avenue,
Ascot, Bulawayo,
Zimbabwe

Journal of Pharmacognosy and Phytotherapy

Table of Contents: Volume 8 Number 5 May 2016

ARTICLES

Design and optimisation of novel Huperzine A analogues capable of modulating the acetylcholinesterase receptor for the management of Alzheimer's disease 99

Sara Bonavia and Claire Shoemake

Analysis of bioactive chemical compounds of Euphorbia lathyrus using gas chromatography-mass spectrometry and Fourier-transform infrared spectroscopy 109

Azhar Abduameer Sosa, Suhaila Husaein Bagi, and Imad Hadi Hameed

Full Length Research Paper

Design and optimisation of novel Huperzine A analogues capable of modulating the acetylcholinesterase receptor for the management of Alzheimer's disease

Sara Bonavia* and Claire Shoemake

Department of Pharmacy, University of Malta, Msida MSD 2080, Malta.

Received 6 October, 2015; Accepted 4 April, 2016

This is a *de novo* drug design study that aimed to create novel structures based on the alkaloid Huperzine A, capable of inhibiting the acetylcholinesterase (AChE) enzyme ligand binding pocket (AChE_LBP) for the management of Alzheimer's disease. The X-ray crystallographic model of the Torpedo Californica AChE complexed to Huperzine A was identified from the Protein Data Bank (PDB ID 1VOT). Molecular visualisation and modelling was carried out using SYBYL[®] 1.2, *in silico* predicted ligand binding affinity (LBA) was quantified using XSCORE_V1.3 and *de novo* drug design was carried out using LIGBUILDER[®]V1.2. Two seed structures were constructed in SYBYL[®] 1.2 according to a methodology that took into account the relationship between molecular structure and biological activity as described in the literature. Based on SAR data derived from Huperzine A, the points considered to be critical for binding were retained in each seed and planted into the AChE_LBP with growth being allowed according to defined parameters of LIGBUILDER[®]V1.2. The implication of this study consequently is that novel structures compliant to Lipinski's Rule of 5 may be promoted to second level drug design which could lead to identification of novel AChE inhibitors with better potency and a low side effect profile.

Key words: *de novo* drug design, Huperzine A, acetylcholinesterase, Alzheimer's disease, Lipinski's Rule of 5.

INTRODUCTION

Alzheimer's disease is the most common cause of dementia (Akhondzadeh and Abbasi, 2006) characterised by the build-up in the brain of protein rich

plaques and leading to decreased cerebral nerve cell connectivity culminating in the death of nerve cells and loss of brain tissue (Wang et al., 2006a). It is also

*Corresponding author. E-mail: sbon121@gmail.com.

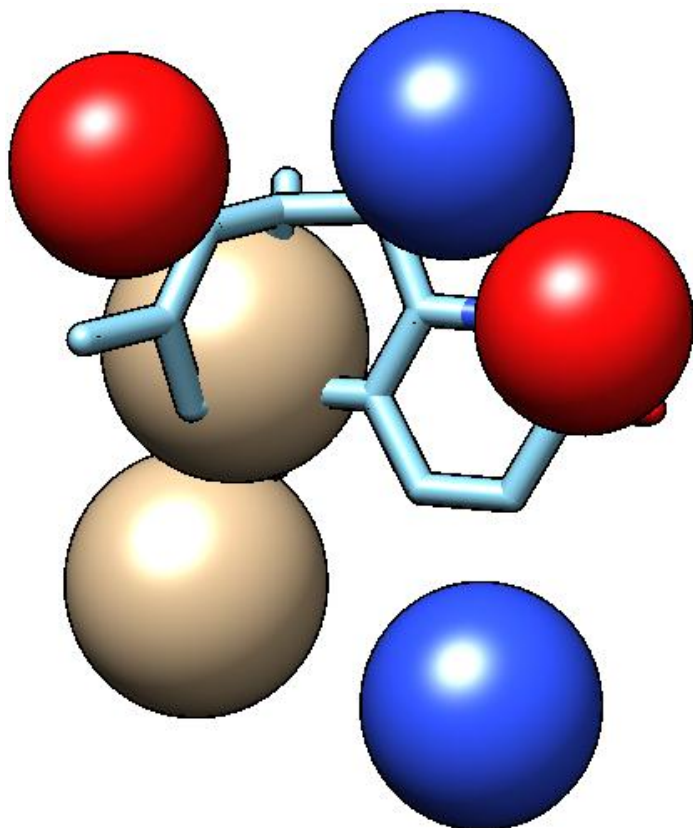


Figure 1. Huperzine A onto its pharmacophore shown in beads rendered in Chimera® v.1.7.

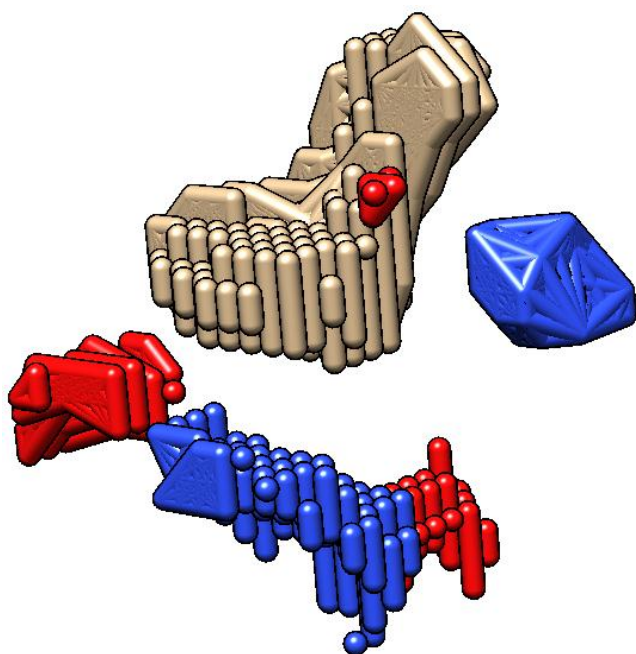


Figure 2. Huperzine A key interaction sites rendered in Chimera® v.1.7 based on the coordinates of PDB ID 1VOT (Raves et al., 1997).

associated with decreased acetylcholine (ACh) levels, due to the fact that this is broken down at a higher than average rate by the acetylcholinesterase (AChE). This also contributes to incomplete transmission of nerve impulses (Picoulin, 2002).

The naturally occurring alkaloid Huperzine A has been shown to be a potent inhibitor of the transport of choline through cholinesterase inhibition consequently resulting in an increase in ACh. AChE inhibition also results in a slower rate of breakdown of acetylcholine and in nerve impulses of strength and duration consequently enhancing cerebral performance (Zangara, 2003).

In this study, an analysis of the binding modality of Huperzine A within the AChE Ligand Binding Pocket and the use of the Huperzine A scaffold to generate analog series of lead molecules for further optimisation using a static algorithm were reported.

METHODOLOGY

Molecular modelling

X-ray crystallographic deposition 1VOT describing the bound coordinates of the Torpedo Californica AChE bound to the nootropic alkaloid Huperzine A was identified from the Protein Data Bank and used as a template for this study (Raves et al., 1997).

Molecular modelling was carried out in Sybyl®-X, Ligand Binding Affinity (LBA) was quantified in X-Score v1.2, and *de novo* ligand generation was carried out using LigBuilder v2.0. VMD® v.1.9 (Humphrey et al., 1996) and Chimera® v.1.7 were used for image generation.

Protein Data Bank crystallographic deposition 1VOT was then read into Sybyl®-X and all water molecules at a distance $\geq 5\text{\AA}$ from the Ligand Binding Pocket were removed. The bound ligand, Huperzine A was extracted from the AChE Ligand Binding Pocket. The now *apo*-AChE and the extracted ligand were saved in PDB and *mol2* format, respectively.

Quantifying the binding affinity (pKd) of huperzine A for the AChE

The *apo*-AChE (saved in *pdb* format) and the extracted ligand (saved in *mol2* format) were used as input files for X-Score® v1.2, which quantified, based on atomic interactions, the affinity (pKd) of the bioactive conformer of Huperzine A for its co-crystallised Ligand Binding Pocket (Wang et al., 1998). This procedure was considered as vital in the establishment of a baseline affinity against which that of the *de novo* generated Huperzine A analogs could be compared.

AChE ligand binding pocket mapping

The POCKET module of LIGBUILDER® v2.0 (Wang et al., 2000) was used to generate a pharmacophore and a 3-Dimensional map of the AChE Ligand Binding Pocket as circumscribed around the bioactive conformation of Huperzine A. Both the general pharmacophoric structure and the 3-Dimensional map of the AChE Ligand Binding Pocket were colour coded by atom type, with hydrogen bond donors and acceptors being coloured blue and red, respectively and with hydrophobic sites being coloured cyan. These are described in Figures 1 and 2, respectively.

The output file in each case was in *pdb* format and could be

Table 1. The 2-dimensional and 3-dimensional structure of Huperzine A as rendered in Symyx[®] Draw 4.0 and VMD[®] v1.9, along with its predicted *in silico* ligand binding affinity to its cognate receptor 1VOT, as calculated in X-Score[®] v1.3.

2-Dimensional Structure	3-Dimensional Structure	Predicted <i>in silico</i> LBA within cognate receptor
Huperzine A within 1VOT		
		HPScore $-\log(K_d) = 6.41$ HMScore $-\log(K_d) = 6.41$ HSScore $-\log(K_d) = 6.54$ Predicted average $-\log(K_d) = 6.45$ Predicted binding energy = -8.80 kcal/mol

visualised in VMD[®] v.1.9 (Humphrey et al., 1996) and Chimera[®] v.1.7. This process was important because it established the pharmacophoric space available for *de novo* ligand construction, as well as the general pharmacophoric structure to which all the *de novo* generated ligands must necessarily comply for efficient binding.

Seed structure construction

A seed structure is essentially a molecular scaffold that is capable of sustaining molecular growth at user directed pre-designated growing sites. For this study, two seed structures were constructed in Sybyl[®]-X according to a methodology that took into account the relationship between molecular structure and biological activity as described in the literature. Seed A was created by removing the methyl group at the 15-position and the carbon group at the 14-position thereby opening the last ring of Huperzine A.

Seed B was created by removing the fused cyclic rings and retaining solely the aromatic ring bearing the carbonyl group and two methyl groups at the 6 and 12 positions. The carbonyl group was retained in both seeds because the pyridone oxygen forms a strong hydrogen bond with a protein residue of the ligand binding pocket. In Seed A, atoms 8 and 13 were designated as growing sites (*H.spc*) whereas in Seed B, atoms 6 and 12 were designated as growing sites (*H.spc*).

de Novo ligand design

The modelled seed structures were successively docked into the AChE Ligand Binding Pocket 3-Dimensional map, with which molecular growth was sustained according to the generic algorithm embedded in the GROW module of LigBuilder[®]V2.0.

The PROCESS module of LigBuilder[®]V2.0 was used to organise the *de novo* generated structured into families based on pharmacophoric similarity, and ranked in order of Ligand Binding

Affinity (pKd).

RESULTS

The *in silico* LBA (pKd) of Huperzine A to its cognate receptor was predicted to be 6.45 as shown in Table 1. The algorithm embedded in the PROCESS module of LIGBUILDER[®]V2.0. This process resulted in 200 and 600 molecules to be generated from Seeds A and B, respectively. These *de novo* structures were divided into a number of families whose *in silico* affinity (pKd), molecular weight (Daltons/Da) and logP are displayed in Figures 3 to 8, respectively. Each molecular structure was assessed for Lipinski rule of 5 (predictors of *in vivo* bioavailability) rule compliance (Lipinski et al., 1997). The pKd for the *de novo* molecules ranged from 6.30 to 10, while molecular weight ranged from 300 to 526 and the LogP ranged from 3 to 5.99. A summary of all the values in each seed may be seen in Table 2.

DISCUSSION

All 15 molecules chosen from Seed A and all 45 molecules chosen from Seed B were Lipinski rule compliant. In an ideal scenario, the molecules with the highest LBA (pKd) would also have the lowest LBE (kcal mol⁻¹). The best molecule from the top 15 molecules chosen from Seed A is molecule number 6 having a pKd of 8.82 and a LBE of 126.999 kcal mol⁻¹. Moreover, the

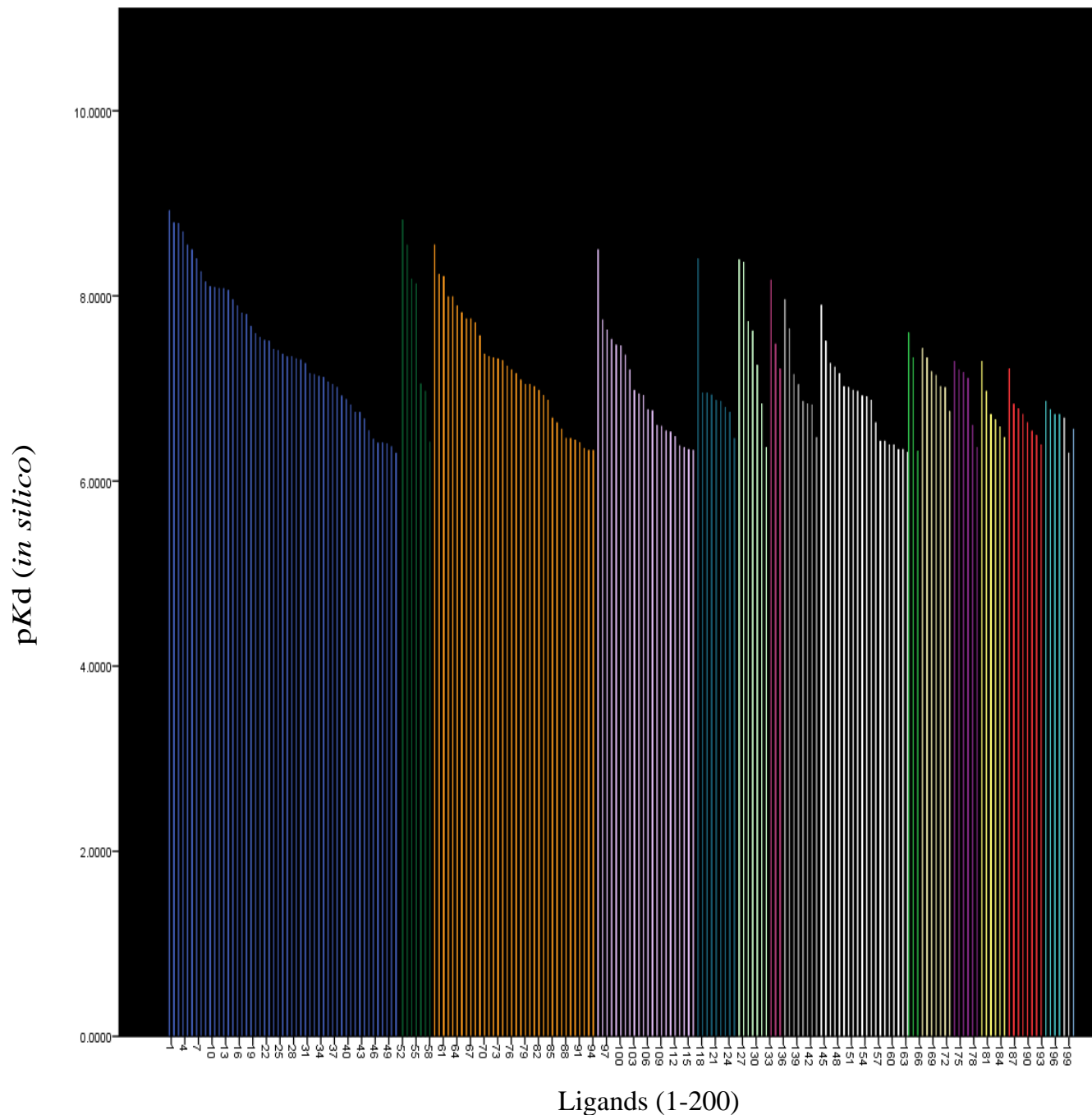


Figure 3. A graph showing the pKd (*in silico*) for the 200 *de novo* designed ligands from Seed A; the 17 different colours imply the 17 family series.

best molecule from the top 45 molecules chosen from Seed B is molecule number 3 having a pKd of 9.37 and a LBE of 45.796 kcal mol⁻¹. The binding poses of molecules 6 and 4 are superimposed onto the bound co-ordinates of Huperzine A as shown in Figures 9 and 10.

From this *de novo* study, the following relationships between structure and activity have been identified:

1) Ligands having two aromatic rings connected by an

aliphatic chain have a high LBA (pKd) and a low LBE (kcal mol⁻¹). This was evident from molecules generated from Seed B.

2) Molecules with an aromatic ring directly attached to a pyridine ring bearing a negatively charged oxygen atom have been observed to have a lower LBA (pKd) and a higher LBE (kcal mol⁻¹). This was apparent from ligands generated from Seed A.

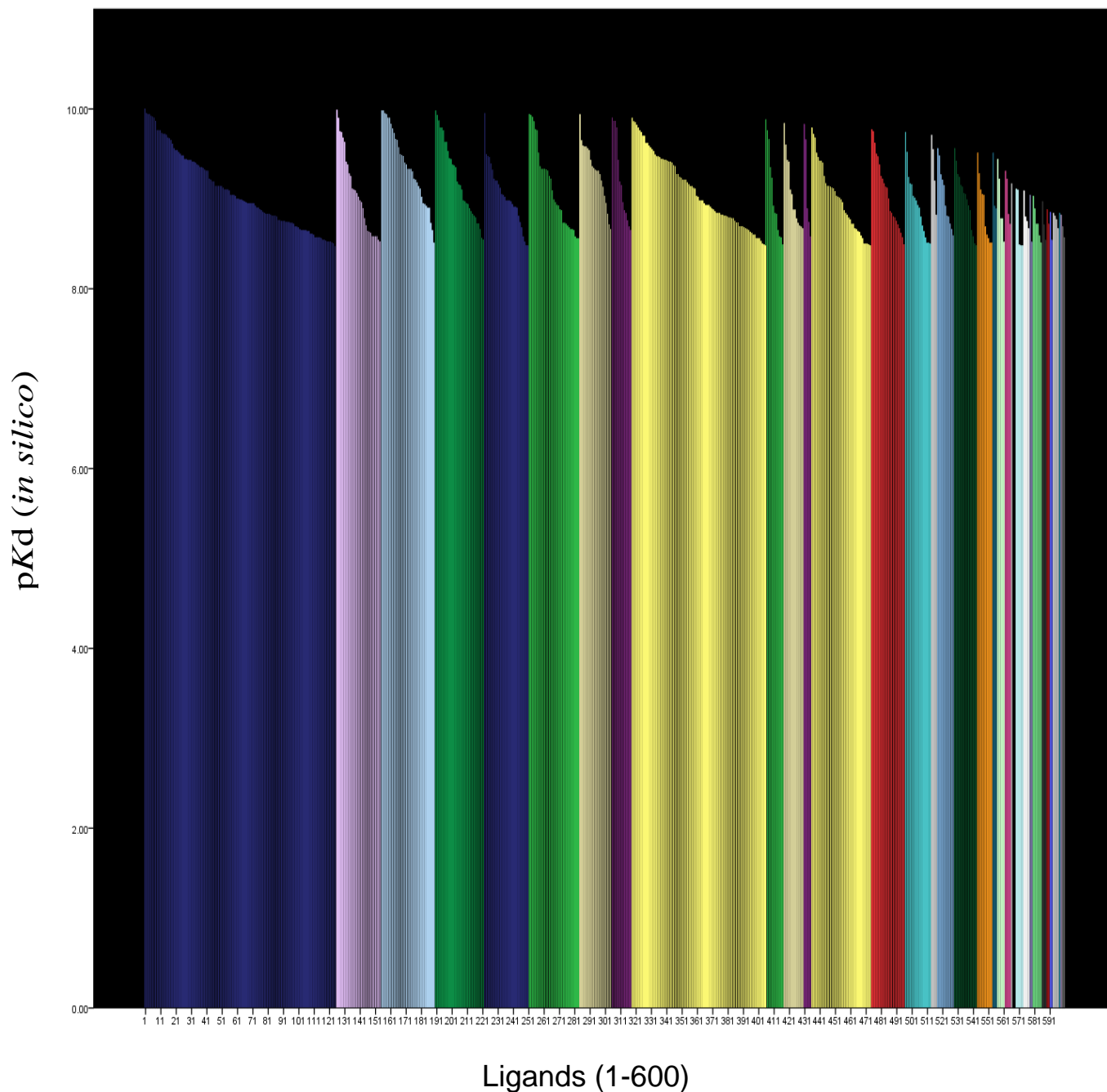


Figure 4. A graph showing the pK_d (*in silico*) for the 600 *de novo* designed ligands from Seed B; the 35 different colours imply the 35 family series.

(3) Ligands with lateral branching ending in an acidic group (specifically the carboxyl group) from the pyridine bearing the carbonyl group have a higher LBA (pK_d) than those which did not have an acidic group.

(4) Molecules having an aromatic ring linked to a pyridine bearing a negatively charged oxygen group exhibited a lower LBA (pK_d) than molecules not having a negatively charged oxygen group connected to the pyridine ring.

(5) Ligands having an aromatic ring bearing a carboxylate anion had a higher LBA (pK_d) than those without the

carboxylate anion.

The implication of this study is that all the novel molecules sampled from both seeds which are also compliant to Lipinski's Rule of 5, are candidates for subsequent iterative rounds of rational drug design and *in vitro* validation.

The best two ligands identified from this study may be considered as viable leads for further optimisation studies. Comparative molecular dynamics studies could shed further light on the way that these ligands interact

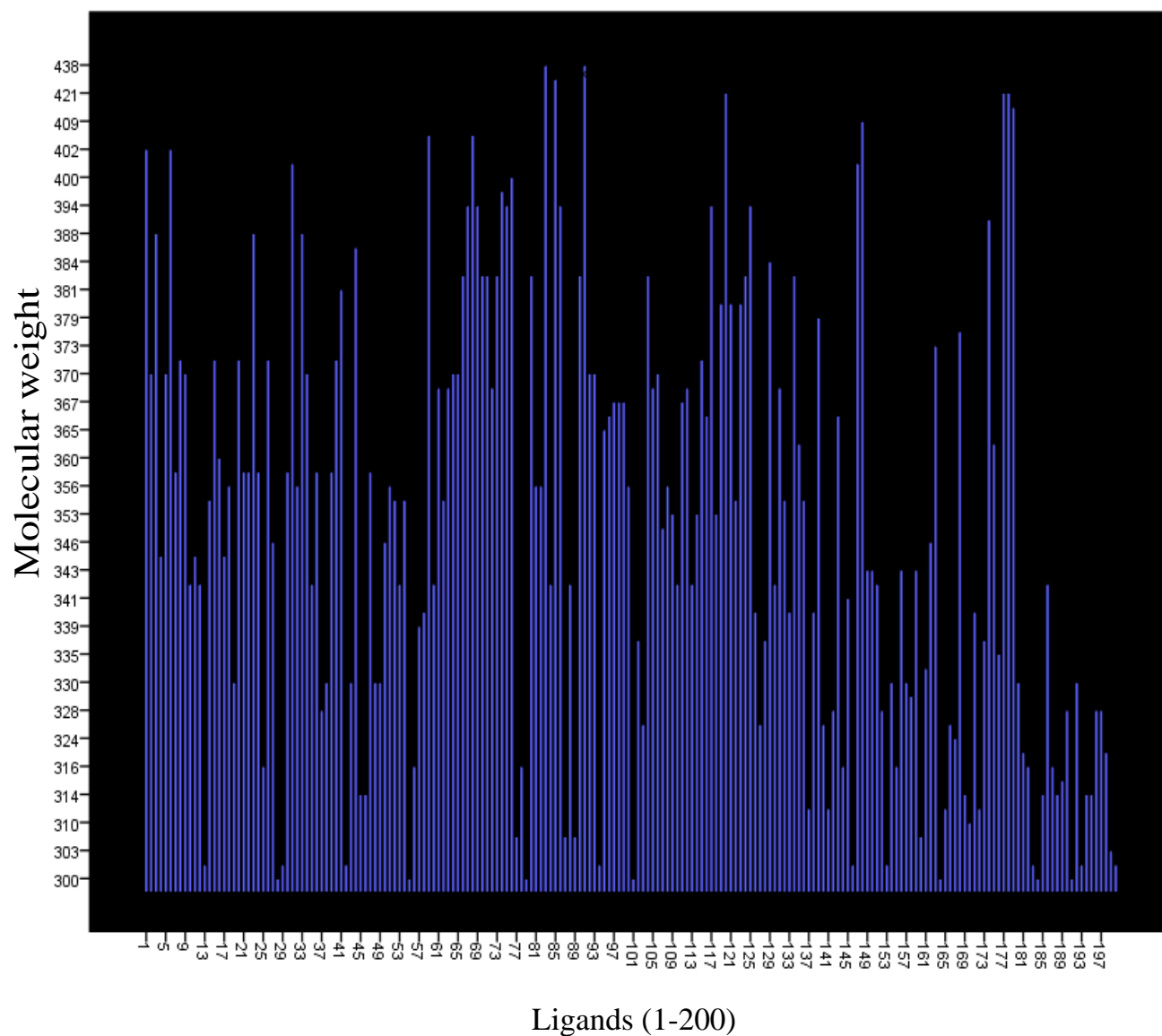


Figure 5. A graph showing the molecular weight for the 200 *de novo* designed ligands from Seed A. All ligands have a molecular weight of less than 500 and therefore are Lipinski rule of 5 compliant with respect to molecular weight only.

Table 2. Summary of important parameters of all the *de novo* molecules generated within LigBuilder® v2.0.

AChE_LBP	Seed A	Seed B
Total number of molecules	200	600
No. of families	17	35
Maximum number of molecules per family	51	125
Minimum number of molecules per family	1	1
Maximum pKd	8.92	10
Minimum pKd	6.30	8.47
Maximum molecular weight	438	526
Minimum molecular weight	300	326
Maximum LogP	5.43	5.99
Minimum LogP	3	3.01

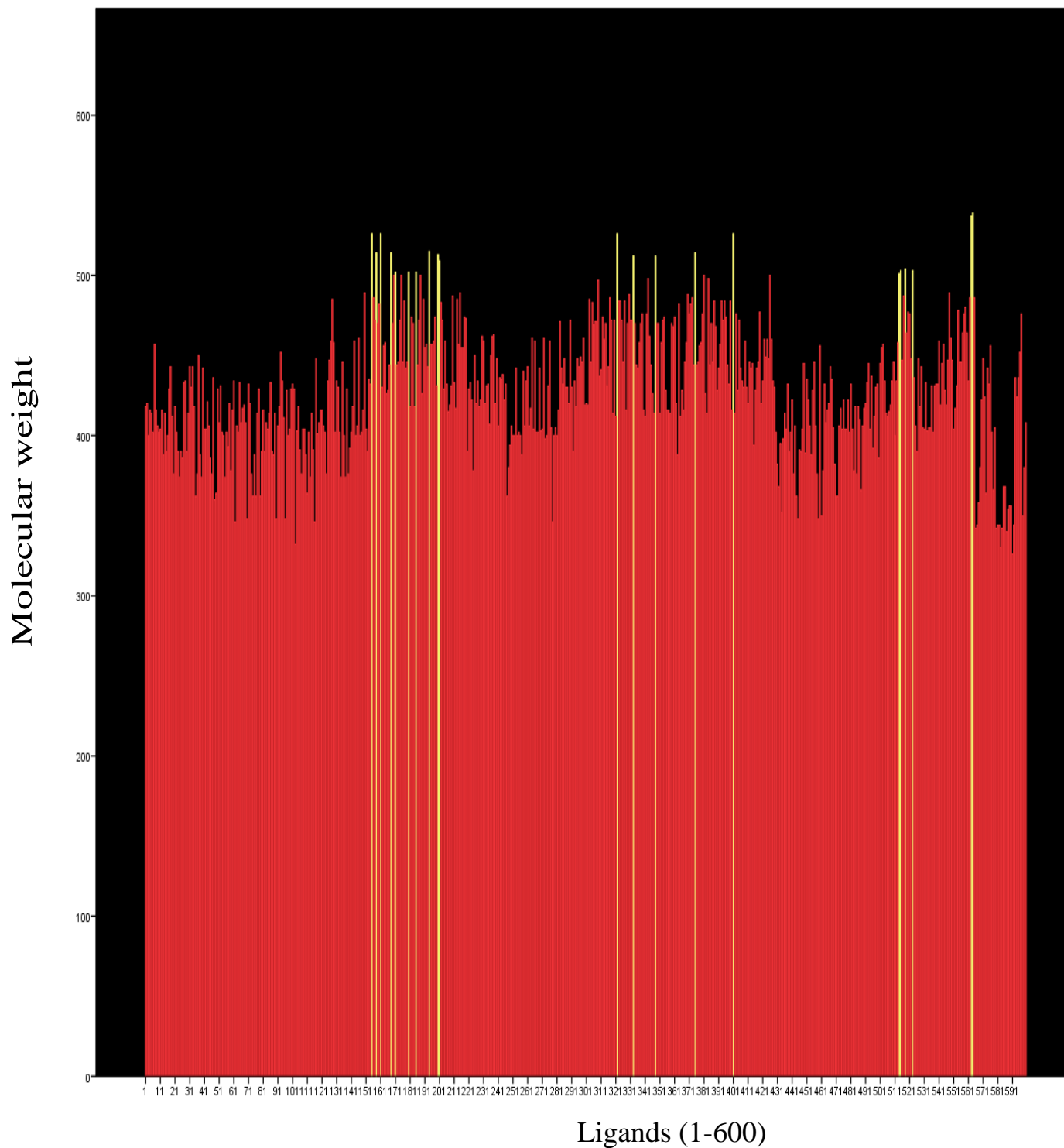


Figure 6. A graph showing the molecular weight for the 600 *de novo* designed ligands from Seed B. The red colour indicates a molecular weight of less than 500 and therefore these ligands are Lipinski rule of 5 compliant with respect to molecular weight only. The yellow colour indicates a molecular weight exceeding 500 and thus such ligands are not Lipinski rule of 5 compliant with respect to molecular weight only.

with the AChE Ligand Binding Pocket relative to Huperzine A, with Principal Component Analysis indicating the most significant ligand driven

conformational changes which could be exploited in *in silico* attempts to identify novel entities with higher LBAs(pKd) and lower LBEs (kcal mol^{-1}). This could lead

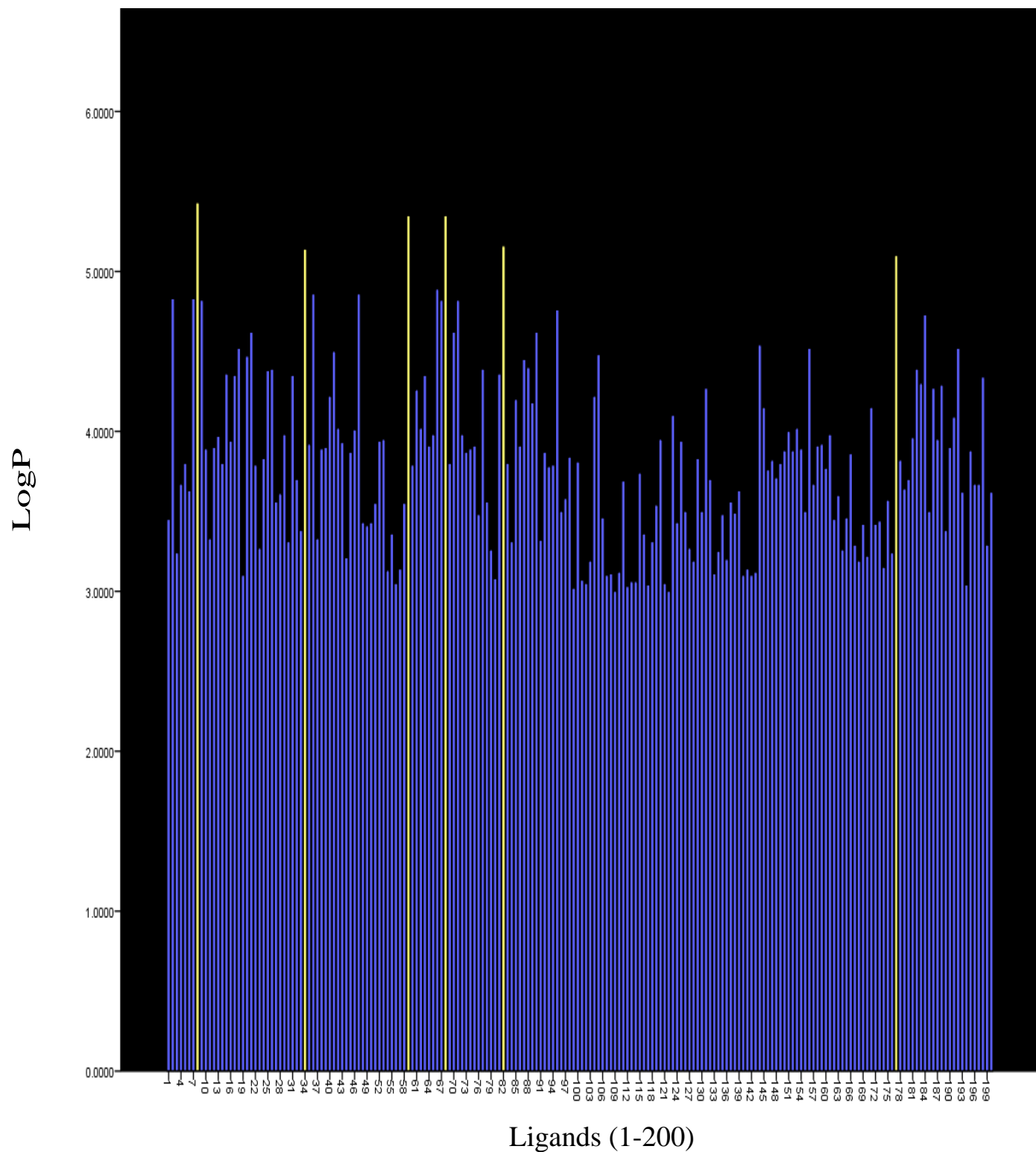


Figure 7. A graph showing the value of LogP for the 200 *de novo* ligands generated from Seed A. The yellow colour indicates a value of more than 5 and therefore such molecules are non-compliant with the Lipinski Rule of 5 with respect to LogP only.

to the identification of innovative AChE inhibitors with better potency and a low side effect profile. AChE

inhibitors will continue to be developed, because this class of drugs has shown promise in symptomatic

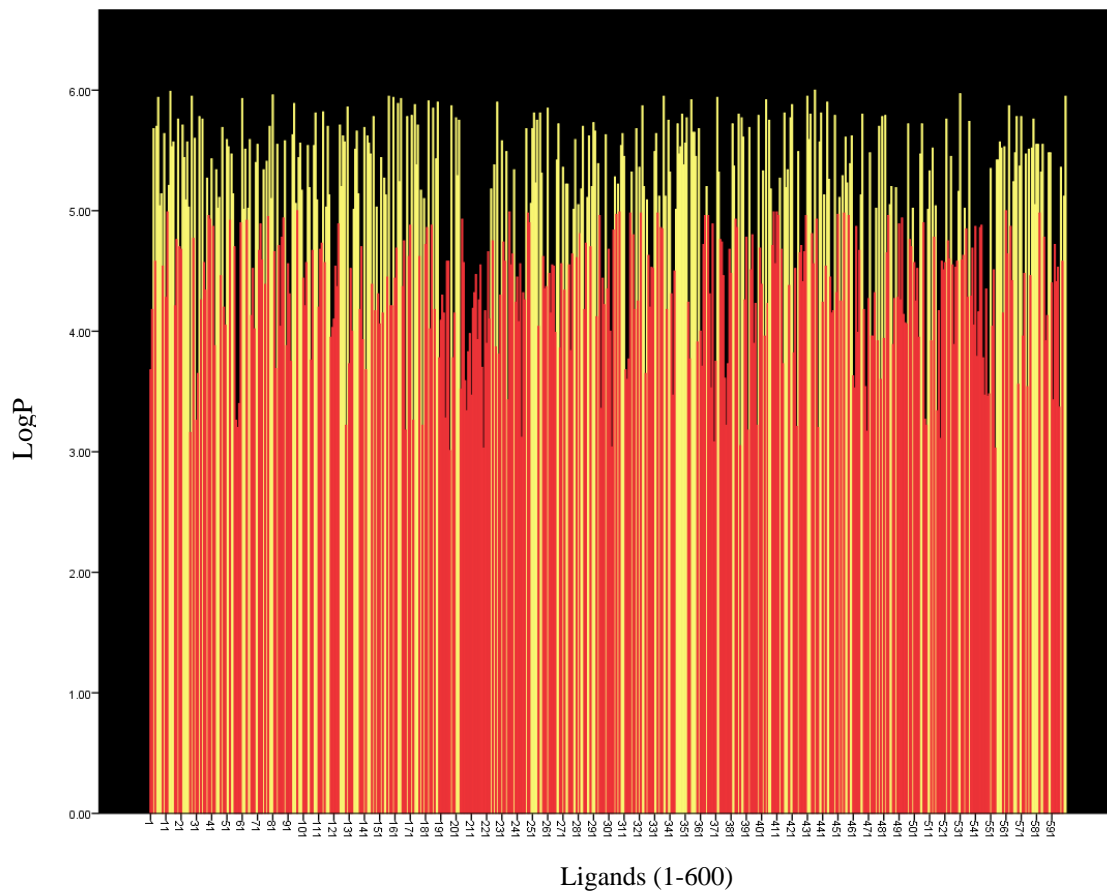


Figure 8. A graph showing the value of LogP for the 600 *de novo* ligands generated from Seed B. The yellow colour indicates a value of more than 5 and therefore such molecules are non-compliant with the Lipinski Rule of 5 with respect to LogP only.

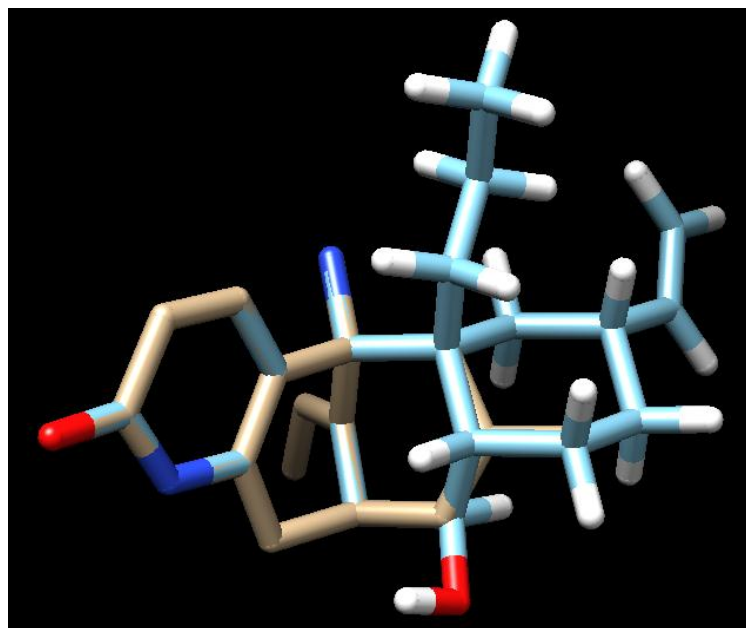


Figure 9. Superimposition of Molecule 6 (shown in light blue and white) onto Huperzine A (shown according to molecular type).

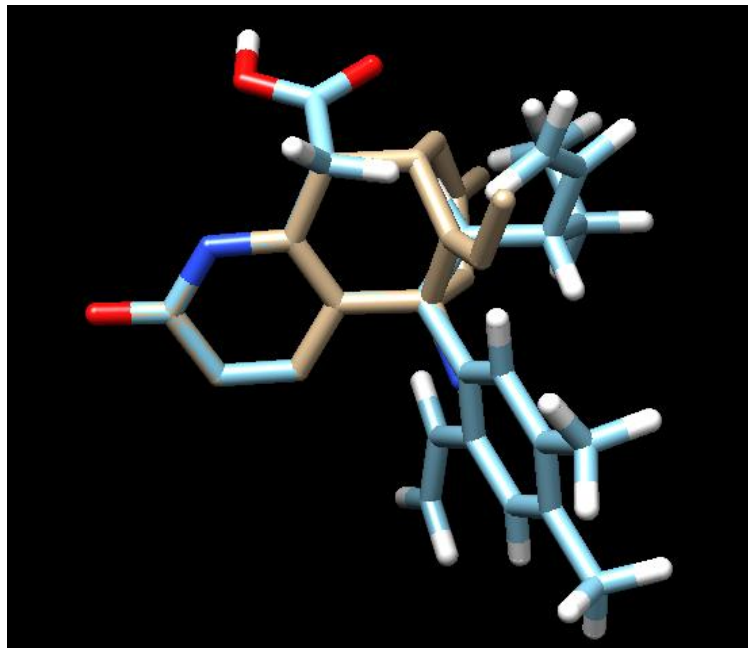


Figure 10. Superimposition of Molecule 4 (shown in light blue and white) onto Huperzine A (shown according to molecular type).

therapy (Mehta et al., 2011).

Conflict of interest

The authors have not declared any conflict of interest

ACKNOWLEDGEMENT

"This submission is sponsored by APL Swift Services (Malta) Limited, a subsidiary of Aurobindo Pharma Limited."

REFERENCES

- Akhondzadeh S, Abbasi SH (2006). Herbal medicine in the treatment of Alzheimer's Disease and Other Dementias. *Am. J. Alzheimers Dis. Other Demen.* 21:113-118.
- Humphrey WF, Dalke A, Schulten K (1996). VMD - Visual Molecular Dynamics. *J. Mol. Graphics* 14:33-38.
- Lipinski CA, Lombardo F, Dominy BW, Feeney PJ (1997). Experimental and computational approaches to estimate solubility and permeability in drug discovery and development settings. *Adv. Drug Delivery Rev.* 23(1-3):3-25.
- Mehta M, Adem A, Sabbagh M (2011). New Acetylcholinesterase Inhibitors for Alzheimer's Disease. *Int. J. Alzheimers Dis.* 728983.

- Picoulin K (2002). *Reversing Alzheimer's Naturally*. Canada: Auburn Hill Publishing Co.
- Raves ML, Harel M, Pang YP, Silman I, Kozikowski AP, Sussman JL (1997). Structure of acetylcholinesterase complexed with the nootropic alkaloid, (-)-huperzine A. *Nat. Struct. Biol.* 4:57-63.
- Wang R, Gao Y, Lai L (2000). LigBuilder: A multi-purpose program for structure-based drug design. *J. Mol. Model.* 6(7-8):498-516.
- Wang R, Liu L, Lai L, Tang Y (1998). Score: A New Empirical Method for Estimating the Binding Affinity of a Protein-Ligand Complex. *J. Mol. Model.* 4:379-394.
- Wang R, Yan H, Tang XC (2006a). Progress in studies of Huperzine A, a natural cholinesterase inhibitor from Chinese herbal medicine. *Acta Pharmacologica Sinica* 27:1-26
- Zangara A (2003). The psychopharmacology of huperzine A: an alkaloid with cognitive enhancing and neuroprotective properties of interest in the treatment of Alzheimer's disease. *Pharmacol. Biochem. Behav.* 75(3):675-86.

Full Length Research Paper

Analysis of bioactive chemical compounds of *Euphorbia lathyris* using gas chromatography-mass spectrometry and Fourier-transform infrared spectroscopy

Azhar Abduameer Sosa¹, Suhaila Husaein Bagi¹, and Imad Hadi Hameed^{2*}

¹College of Education for Women, Al-Qadisiya University, Iraq.

²College of Nursing, Babylon University, Iraq.

Received 29 August, 2015; Accepted 14 March, 2016

The aim of this study was determination the phytochemical composition of methanolic seeds extract of *Euphorbia lathyris*. Gas chromatography-mass spectrometry (GC-MS) analysis of *E. lathyris* revealed the existence of the Carbonic acid, (ethyl)(1,2,4-triazol-1-ylmethyl) diester, 1H-Pyrrole,2,5-dihydro-1-nitroso, Hexanal dimethyl acetal, Isosorbide dinitrate, DL-Arabinose, Cyclopropane,1-fluoro-1-(2-bromoethenyl)-2,2,3,3-tetramethyl, α -D-Glucopyranoside, O- α -D-glucopyranosyl-(1.fwdarw.3)- β -d-fruc, Desulphosinigrin, D-Glucose, 6-O- α -D-galactopyranosyl, Octanoic acid, Benzofuran,2,3-dihydro, 6-Acetyl- β -d-mannose, Estragole, Ascaridole epoxide, 3-Allyl-6-methoxyphenol, 4-Amino-1,5,pentandioic acid, l-Gala-l-ido-octonic lactone, γ -Sitosterol, Tetradecanoic acid, l-(+)-Ascorbic acid 2,6-dihexadecanoate, Estra -1,3,5(10)-trien-17 β -ol, Propanoic acid,2-(3-acetoxy-4,4,14-trimethylandrost-8-en-17-yl), Cis-13-Eicosenoic acid, Eicosanoic acid, 3-Pyridinecarboxylic acid, 2,7,10-tris(acetyloxy)-1,1a,2,3,4,6,7,10, Oleic acid, eicosyl ester, Butanoic acid, 4-chloro-,1,1a,1b,4,4a,5,7a,7b,8,9-decahydro-4a, Ethyl iso-allocholate, Ethyl iso -allocholate, Olean-12-ene-3,15,16,21,22,28-hexol, (3 β ,15 α ,16 α ,21 β ,22 α)- and 2,4,6-Decatrienoic acid,1a,2,5,5a,6,9,10,10a-octahydro-5,5a-dihy. The Fourier-transform infrared spectroscopy (FTIR) analysis of *E. lathyris* seeds proved the presence of alkenes, aliphatic fluoro compounds, alcohols, ethers, carboxylic acids, esters, nitro compounds, alkanes, hydrogen bonded alcohols, and phenols.

Key words: Gas chromatography-mass spectrometry (GC/MS), bioactive compounds, Fourier-transform infrared spectroscopy (FT-IR), *Euphorbia lathyris*.

INTRODUCTION

Medicinal plant parts (roots, leaves, branches/stems, barks, flowers, and fruits) are commonly rich in phenolic

compounds, such as flavonoids, phenolic acids, stilbenes, tannins, coumarins, lignans and lignins (Cai et

*Corresponding author. E-mail: imad_dna@yahoo.com. Tel: 009647716150716.

al., 2004; Altameme et al., 2015a; Al-Marzoqi et al., 2015). The seed of *Euphorbia lathyris* is a traditional Chinese medicine which has been used for the treatment of hydropsy, ascites, anuresis and constipation, amenorrhea, and scabies (Liu et al., 2011). Nowadays, traditional medicinal practices form an integral part of complementary or alternative medicine. Although their efficacy and mechanisms of action have not been tested scientifically in most cases, these simple medicinal preparations often mediate beneficial responses due to their active chemical constituents (Park and Pezzutto, 2002; Corro et al., 2014; Hameed et al., 2015a). In recent years, it was reported that the seeds of *Euphorbia* had a significant effect on leukemia, esophageal carcinoma, and skin cancer (Tapiero et al., 2002; Liu et al., 2011; Al-Marzoqi et al., 2016). The seed of *E. lathyris* is a kind of toxic traditional Chinese medicine, which is characterized by pungent, warm and poisonous in drug properties. It shows several side effects, such as irritation and inflammation intense on the skin, mouth and gastrointestinal tract irritation, carcinogenic, etc. (Buenz et al., 2004; Altameme et al., 2015b). The objective of this study was to analyse the chemical composition of seeds extract from methanol. The phytochemical compound was screened by gas chromatography-mass spectrometry (GC-MS) and Fourier-transform infrared spectroscopy (FT-IR) technique.

MATERIALS AND METHODS

Plant and preparation of extracts

E. lathyris dried seeds were purchased from local market in hilla city, middle of Iraq. After thorough cleaning and removal of foreign materials, the fruits were stored in airtight container to avoid the effect of humidity and then stored at room temperature until further use. About 30 g of the plant sample powdered were soaked in 100 ml methanol for 16 h in a rotatory shaker (Hamza et al., 2015; Hussein et al., 2016a). Whatman No.1 filter paper was used to separate the extract of plant. The filtrates were used for further phytochemical analysis. It was again filtered through sodium sulphate in order to remove the traces of moisture (Altameme et al., 2015c; Hameed et al., 2015b).

Identification of component by GC-MS analysis

The physicochemical properties of *E. lathyris* are shown in Table 1. Interpretation of mass spectroscopy (GC-MS) was conducted by using data base of National Institute Standard and Technology (NIST) having more than 62000 patterns. The spectrum of the unknown component was compared with the spectrum of the known component stored in the NIST library. The identity of the components in the extracts was assigned by the comparison of their retention indices and mass spectra fragmentation patterns with those stored on the computer library and also with published literatures (Hadi et al., 2016; Hameed et al., 2015c; Hussein et al., 2016b). The GC-MS analysis of the plant extract was made in an Agilent 7890 A instrument under computer control at 70 eV. About 1 µl of the methanol extract was injected into the GC-MS using a micro syringe and the scanning was done for 45 min. The fragments obtained were actually charged ions with a certain mass

(Hameed et al., 2015d; Hussein et al., 2016c). Helium gas was used as a carrier as well as an eluent. The flow rate of helium was set to 1 ml/min. The electron gun of mass detector liberated electrons having energy of about 70 eV. The column employed here for the separation of components was Elite 1 (100% dimethyl poly siloxane).

Fourier transform infrared spectrophotometer (FTIR)

The powdered sample of *E. lathyris* specimen was treated for FTIR spectroscopy (Shimadzu, IR Affinity 1, Japan). The sample was run at infrared region between 400 and 4000 nm (Hussein et al., 2016; Jasim et al., 2015).

RESULTS AND DISCUSSION

Gas chromatography and mass spectroscopy analysis of compounds was carried out in methanolic seed extract of *E. lathyris* shown in Table 1. The GC-MS chromatogram of the 31 peaks of the compounds detected is as shown in Figure 1. Chromatogram GC-MS analysis of the methanol extract of *E. lathyris* showed the presence of thirty one major peaks and the components corresponding to the peaks were determined as follows. The first set up peak was determined to be Carbonic acid, (ethyl)(1,2,4-triazol-1-ylmethyl) diester (Figure 2). The next peaks were considered to be 1H-Pyrrole,2,5-dihydro-1-nitroso, Hexanal dimethyl acetal, Isosorbide dinitrate, DL-Arabinose, Cyclopropane,1-fluoro-1-(2-bromoethyl)-2,2,3,3-tetramethyl, α-D-Glucopyranoside, O-α-D-glucopyranosyl - (1.fwdarw.3) - β - d-fruc, Desulphosinigrin, D-Glucose, 6-O-α-D-galactopyranosyl, Octanoic acid, Benzofuran,2,3-dihydro, 6-Acetyl-β-d-mannose, Estragole, Ascaridole epoxide, 3-Allyl-6-methoxyphenol, 4-Amino-1,5,pentandioic acid, l-Gala-l-ido-octonic lactone, γ-Sitosterol, Tetradeconoic acid, l-(+)-Ascorbic acid 2,6-dihexadecanoate, Estra-1,3,5(10)-trien-17β-ol, Propanoic acid,2-(3-acetoxy-4,4,14-trimethylandro-8-en-17-yl), Cis-13-Eicosenoic acid, Eicosanoic acid, 3-Pyridinecarboxylic acid, 2,7,10-tris(acetyloxy)-1,1a,2,3,4,6,7,10, Oleic acid, eicosyl ester, Butanoic acid, 4-chloro-,1,1a,1b,4,4a,5,7a,7b,8,9-decahydro-4a, Ethyl iso-allocholate, Ethyl iso - allocholate, Olean-12-ene-3,15,16,21,22,28-hexol, (3β,15α,16α,21β,22α)- and 2,4,6-Decatrienoic acid,1a,2,5,5a,6,9,10,10a-octahydro-5,5a-dihy (Figures 3 to 31). The FTIR analysis of *E. lathyris* seeds proved the presence of alkenes, aliphatic fluoro compounds, alcohols, ethers, carboxylic acids, esters, nitro compounds, alkanes, hydrogen bonded alcohols and phenols which shows major peaks at 837.11, 918.12, 1037.70, 1145.72, 1232.51, 1261.45, 1317.38, 1409.96, 1519.91, 1625.99, 1741.72, 2682.98, 2854.65, 2924.09, 3082.25, and 3275.13 (Table 2 and Figure 32). *E. lathyris* L. active for disinfection is an herbaceous plant of Euphorbiaceae and has been extensively researched in the field of medicine. Phenolic compounds were isolated and identified from *E. lathyris* using RP-HPLC under the

Table 1. Major phytochemical compounds identified in methanolic extract of *Euphorbia lathyris*.

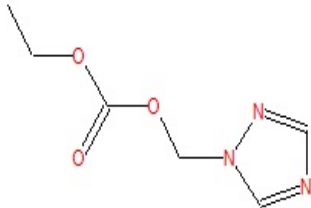
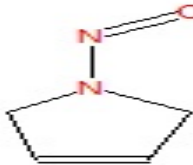
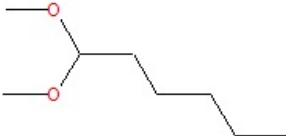
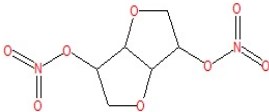
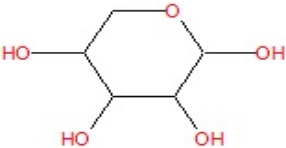
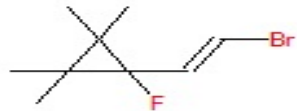
S/N	Phytochemical compound	RT (min)	Molecular Weight	Exact mass	Chemical structure	Pharmacological actions
1	Carbonic acid, (ethyl)(1,2,4-triazol-1-ylmethyl) diester	3.259	171	171.064391		Pharmacological activities such as anti-microbial, anti-inflammatory
2	1H-Pyrrole,2,5-dihydro-1-nitroso-	3.367	98	98.0480127		Antibacterial, antiviral, anticonvulsant and analgesic
3	Hexanal dimethyl acetal	3.533	146	146.13068		Antiviral and anti-inflammatory
4	Isosorbide dinitrate	4.546	236	236.028066		Relaxation
5	DL-Arabinose	4.878	150	150.052823		Anti-tumor activity
6	Cyclopropane,1-fluoro-1-(2-bromoethenyl)-2,2,3,3-tetramethyl-	5.010	220	220.026291		Many medicinal activities, which included anti-cancer and anti-cardiovascular

Table 1. cont'd

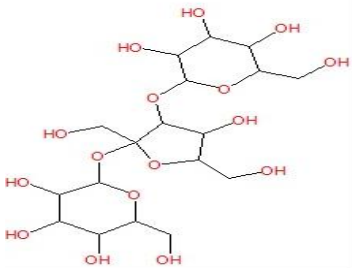
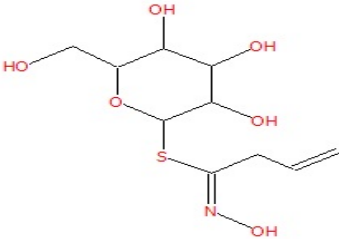
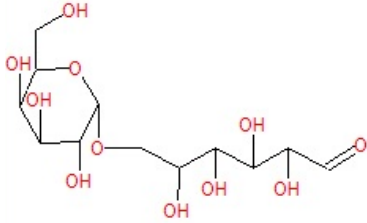
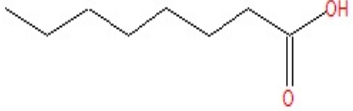
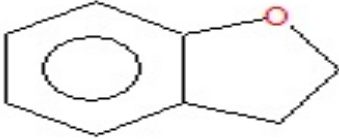
7	α -D-Glucopyranoside, O- α -D-glucopyranosyl-(1.fwdarw.3)- β -d-fruc	5.261	504	504.169035		Anti-diabetic activity and anti-tumour
8	Desulphosinigrin	5.313	279	279.077658		Antibacterial activity
9	D-Glucose, 6-O- α -D-galactopyranosyl	5.782	342	342.11621		Anti-trypanosomal activity
10	Octanoic acid	6.137	144	144.115029		Anti-bacterial activity
11	Benzofuran,2,3-dihydro-	6.715	120	120.0575147		Anti-HIV, anticancer, antibacterial, and antifungal activities

Table 1. cont'd

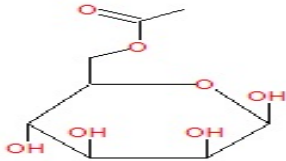
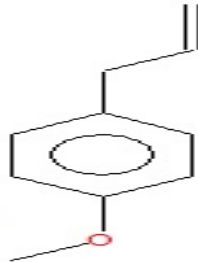
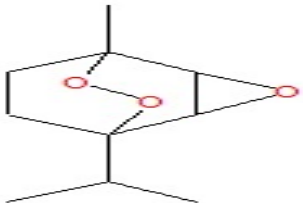
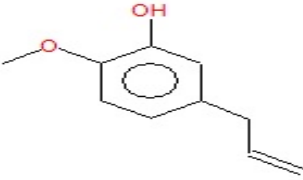
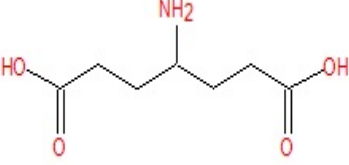
12	6-Acetyl- β -d-mannose	6.984	222	222.073953	 <p>The structure shows a six-membered pyranose ring in its chair conformation. The hydroxyl groups at C2, C3, and C4 are in the equatorial position. At C6, there is an acetyl group (-COCH₃) attached to the CH₂ group.</p>	Anti-inflammatory and anti-oxidant
13	Estragole	7.481	148	148.088815	 <p>The structure consists of a benzene ring with a methoxy group (-OCH₃) at the para position and an allyl group (-CH₂-CH=CH₂) at the other para position.</p>	Estragole has been shown to have an anti-inflammatory activity
14	Ascaridole epoxide	7.727	184	184.109944	 <p>The structure is a bicyclic system with a six-membered ring fused to a five-membered ring. It features an epoxide group on the six-membered ring and a methyl group on the five-membered ring.</p>	Anti-inflammatory
15	3-Allyl-6-methoxyphenol	8.443	164	164.08373	 <p>The structure is a benzene ring with a hydroxyl group (-OH) at the 1-position, a methoxy group (-OCH₃) at the 6-position, and an allyl group (-CH₂-CH=CH₂) at the 3-position.</p>	Anticancer activity
16	4-Amino-1,5-pentandioic acid	9.564	175	175.084458	 <p>The structure is a five-carbon chain with carboxylic acid groups at C1 and C5, and an amino group (-NH₂) at C4.</p>	Anti-cancer agent

Table 1. cont'd

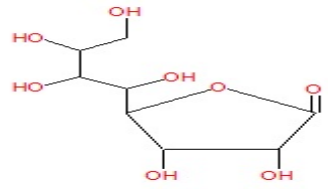
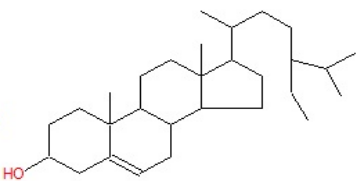
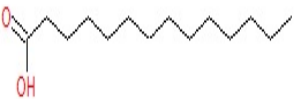
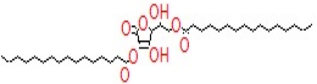
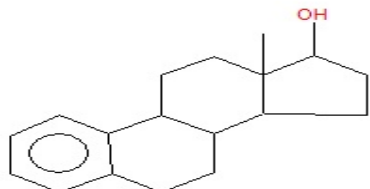
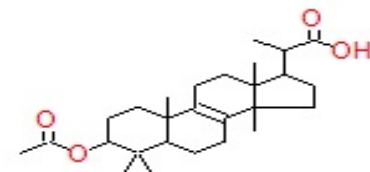
17	l-Gala-l-ido-octonic lactone	10.734	238	238.068868		Antibacterial activity against <i>Pseudomonas aerogenosa</i>
18	γ -Sitosterol	15.023	414	414.386166		Anti-inflammatory activity
19	Tetradecanoic acid	13.455	228	228.20893		Antimicrobial, antispasmodic and <i>anti-inflammatory</i> effects
20	l-(+)-Ascorbic acid 2,6-dihexadecanoate	15.486	652	652.49142		antioxidant
21	Estra -1,3,5(10)-trien-17 β -ol	16.007	256	256.182714		New chemical compound
22	Propanoic acid ,2-(3-acetoxy-4,4,14-trimethylandro-8-en-17-yl)-	16.745	430	430.30831		Anti-microbial and anti-tumor effects.

Table 1. cont'd

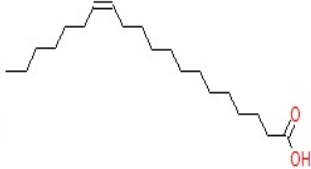
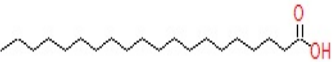
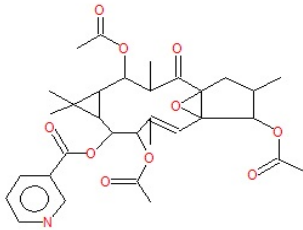
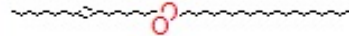
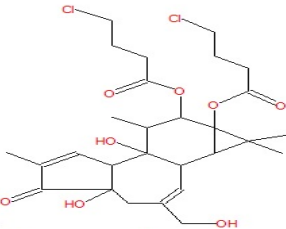
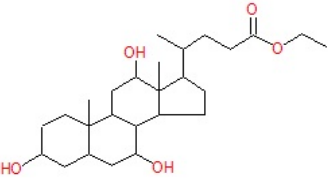
23	Cis-13-Eicosenoic acid	18.914	310	310.28718		Anti-inflammatory activity
24	Eicosanoic acid	19.051	312	312.30283		Anti-inflammatory effects
25	3-Pyrinecarboxylic acid, 2,7,10-tris(acetyloxy)-1,1a,2,3,4,6,7,10	19.246	597	597.257397		New chemical compound
26	Oleic acid, eicosyl ester	20.339	562	562.568882		Anti-Candida activity
27	Butanoic acid, 4-chloro-, 1,1a,1b,4,4a,5,7a,7b,8,9-decahydro-4a	21.083	572	572.194374		Antiviral, antitumor, anti-HIV and antinociceptive activities
28	Ethyl iso -allocholate	21.134	436	436.318874		Anti-inflammatory activity

Table 1. cont'd

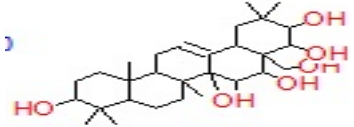
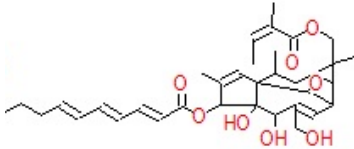
29	Olean-12-ene-3,15,16,21,22,28-hexol, (3 β ,15 α ,16 α ,21 β ,22 α)-	21.603	506	506.360739		Anti-inflammatory
30	2,4,6-Decatrienoic acid, 1a,2,5,5a,6,9,10,10a-octahydro-5,5a-dihy	21.878	594	594.319267		Anticancer

Table 2. FT-IR peak values of *Euphorbia lathyris*.

No.	Peak (Wave number cm^{-1})	Intensity	Bond	Functional group assignment	Group frequency
1	659.66	59.626	-	Unknown	-
2	837.11	74.522	C-H	Alkenes	675-995
3	898.83	73.438	C-H	Alkenes	675-995
4	918.12	73.336	C-H	Alkenes	675-995
5	1037.7	54.275	C-F stretch	Aliphatic fluoro compounds	1000-1050
6	1145.7	65.485	C-O	Alcohols, Ethers, Carboxylic acids, Esters	1050-1300
7	1232.5	69.798	C-O	Alcohols, Ethers, Carboxylic acids, Esters	1050-1300
8	1261.5	72.924	C-O	Alcohols, Ethers, Carboxylic acids, Esters	1050-1300
9	1317.4	73.54	NO ₂	Nitro Compounds	1300-1370
10	1377.2	73.54	C-H	Alkanes	1340-1470
11	1410	74.741	C-H	Alkanes	1340-1470
12	1456.3	74.929	C-H	Alkanes	1340-1470
13	1519.9	70.721	-	Unknown	-
14	1626	62.255	-	Unknown	-
15	1741.7	79.565	-	Unknown	-
16	2683	92.491	-	Unknown	-
17	2854.7	80.11	C-H	Alkanes	2850-2970
18	2924.1	73.299	C-H	Alkanes	2850-2970
19	3082.3	86.714	H-O	H-bonded H-X group	2500-3500
20	3275.1	79.255	O-H	Hydrogen bonded Alcohols, Phenols	3200-3600

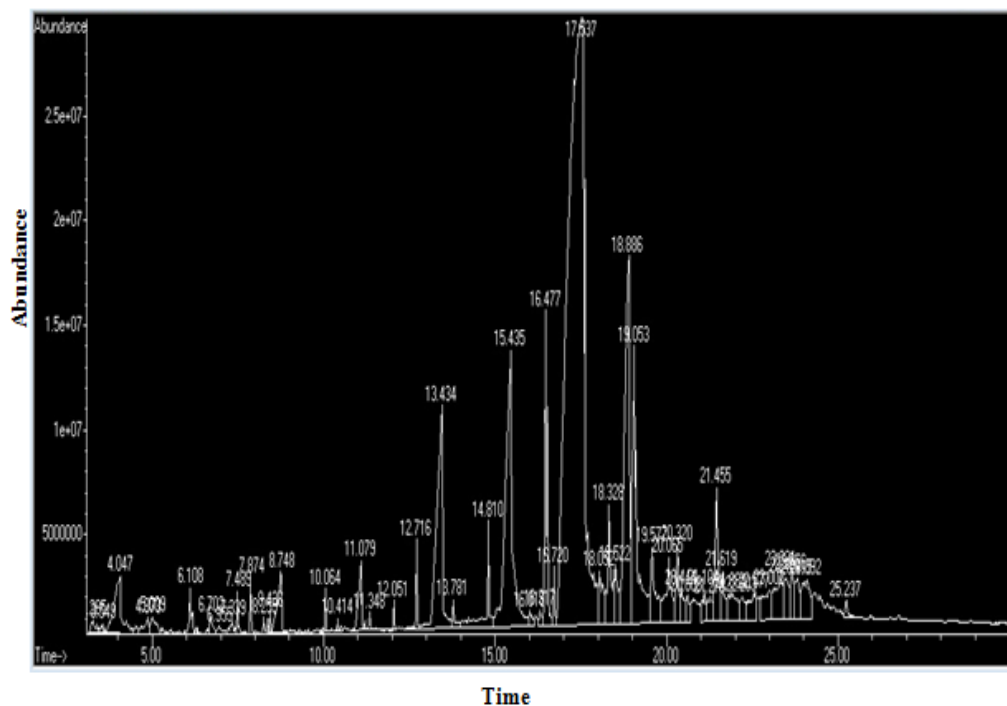


Figure 1. GC-MS chromatogram of methanolic extract of *Euphorbia lathyris*.

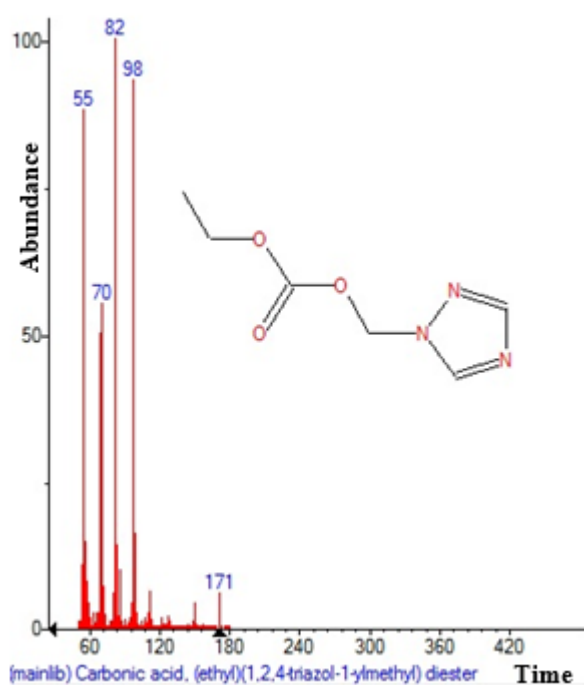


Figure 2. Structure of Carbonic acid, (ethyl)(1,2,4-triazol-1-ylmethyl) diester with 3.259 (RT) present in *Euphorbia lathyris*.

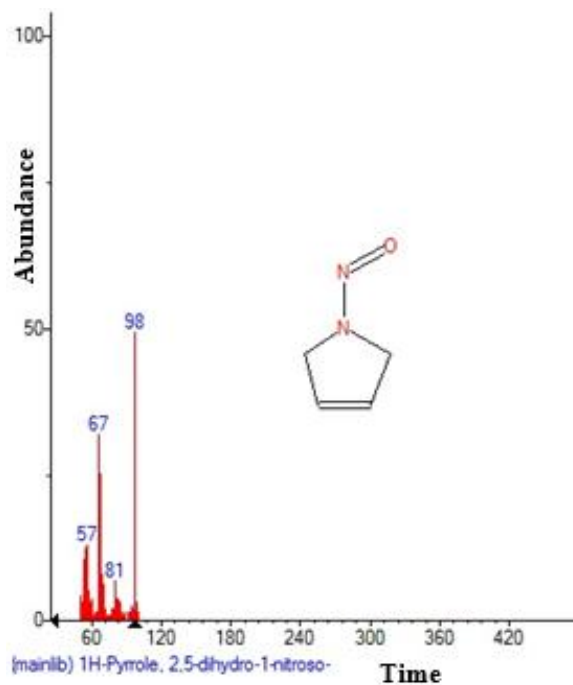


Figure 3. Structure of 1H-Pyrrole, 2,5-dihydro-1-nitroso- with 3.367 (RT) present in *Euphorbia lathyris*.

chromatographic conditions (Shahat et al., 2003; Reddy et al., 2003). *E. lathyris* L. oil (ELO) contains large

amounts of FFAs and needs to determine acid value (Wei et al., 2007; Liu et al., 2011).

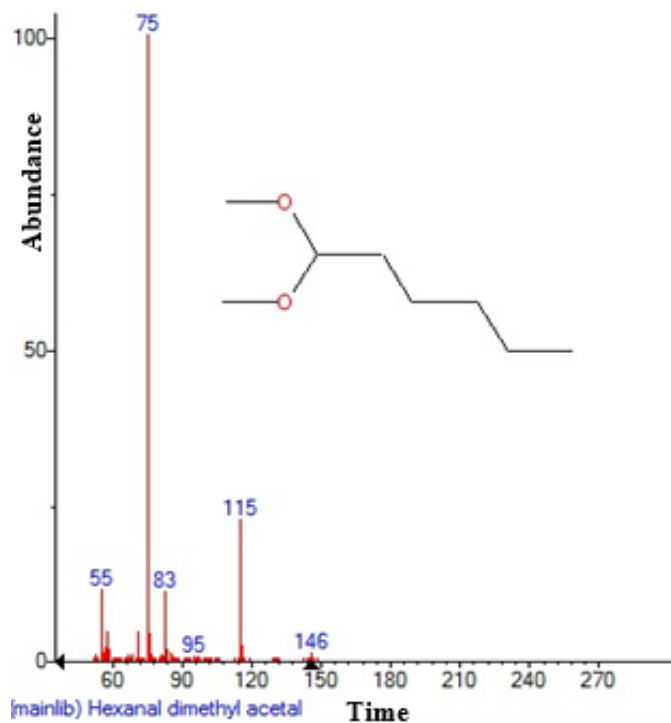


Figure 4. Structure of Hexanal dimethyl acetal with 3.533 (RT) present in *Euphorbia lathyris*.

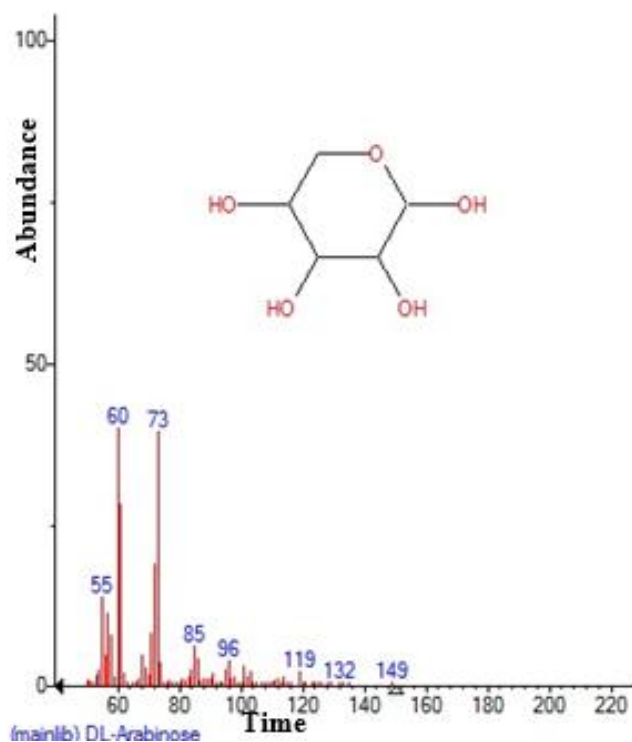


Figure 6. Structure of DL-Arabinose with 4.878 (RT) present in *Euphorbia lathyris*

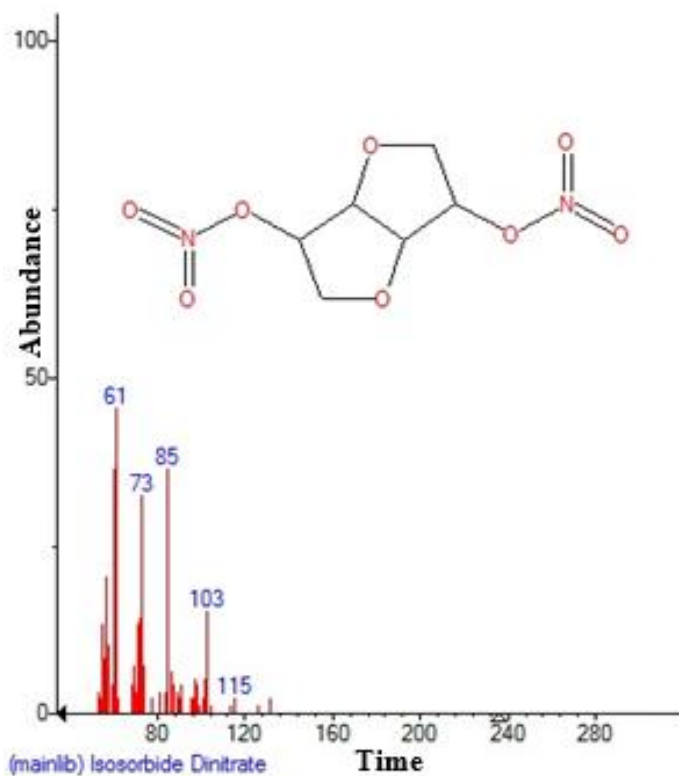


Figure 5. Structure of Isosorbide dinitrate with 4.546 (RT) present in *Euphorbia lathyris*.

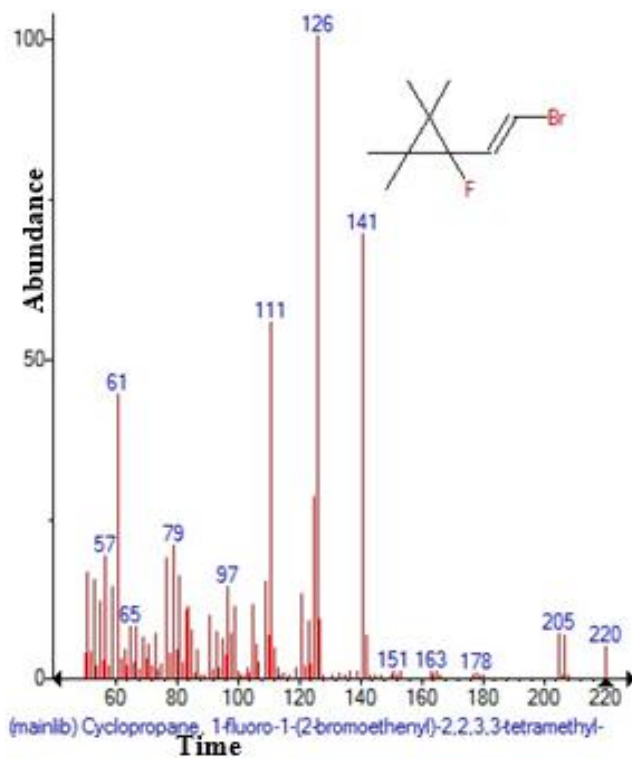


Figure 7. Structure of Cyclopropane ,1-fluoro-1-(2-bromoethyl)-2,2,3,3-tetramethyl with 5.010 (RT) present in *Euphorbia lathyris*.

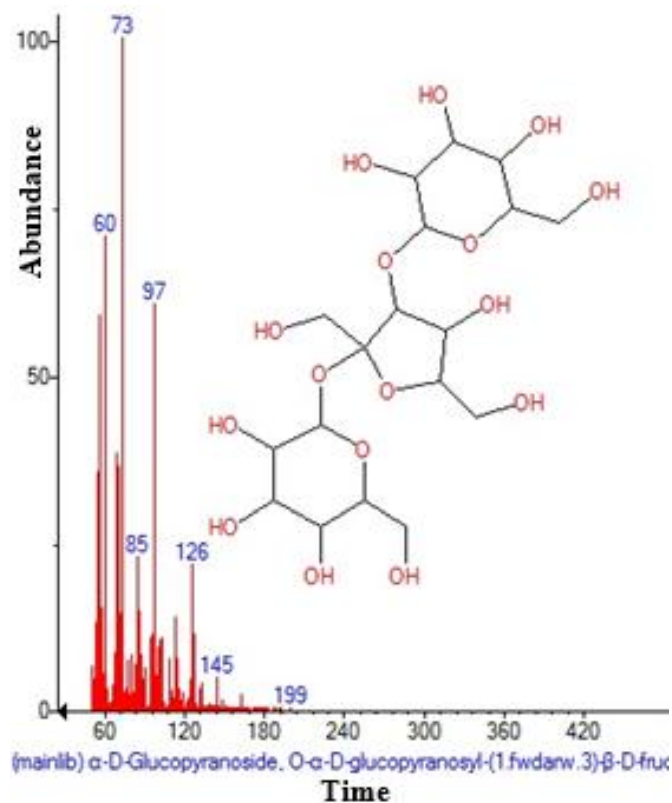


Figure 8. Structure of α -D-Glucopyranoside, O- α -D-glucopyranosyl-(1.fwdarw.3)- β -d-fruc with 5.261 (RT) present in *Euphorbia lathyris*.

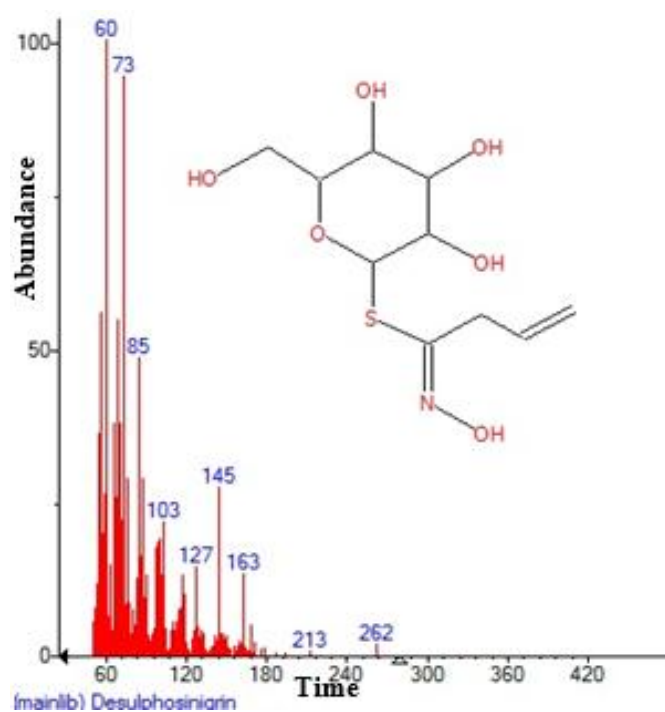


Figure 9. Structure of Desulphosiniarin with 5.313 (RT) present in *Euphorbia lathyris*.

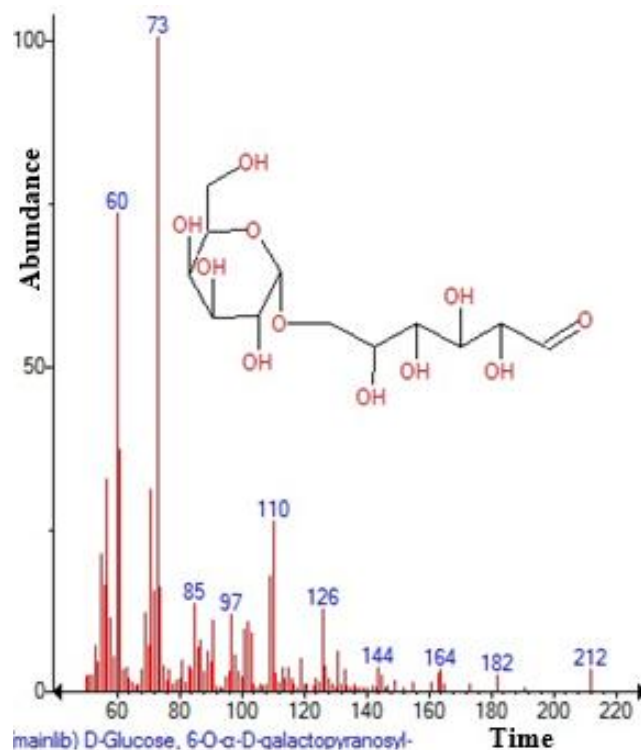


Figure 10. Structure of D-Glucose, 6-O- α -D-galactopyranosyl with 5.782 (RT) present in *Euphorbia lathyris*.

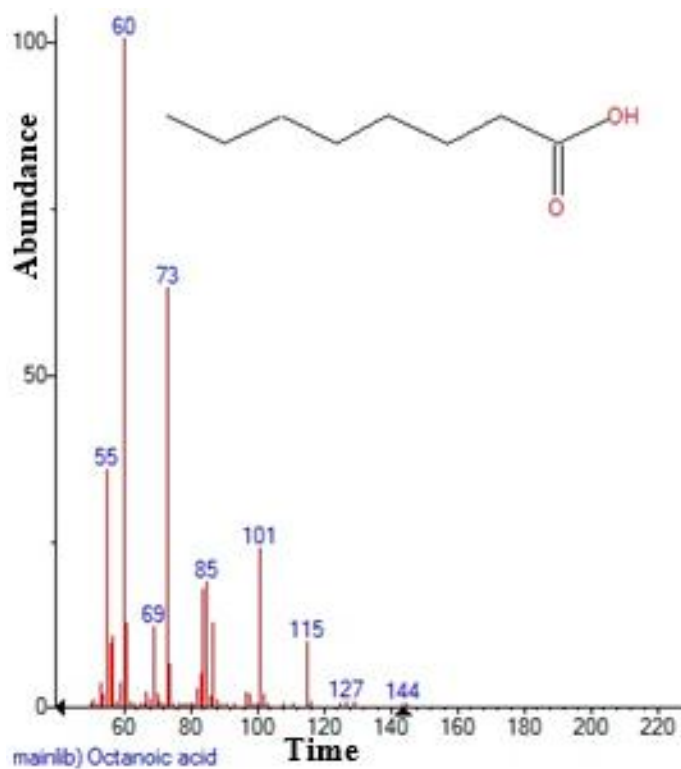


Figure 11. Structure of Octanoic acid with 6.137 (RT) present in *Euphorbia lathyris*.

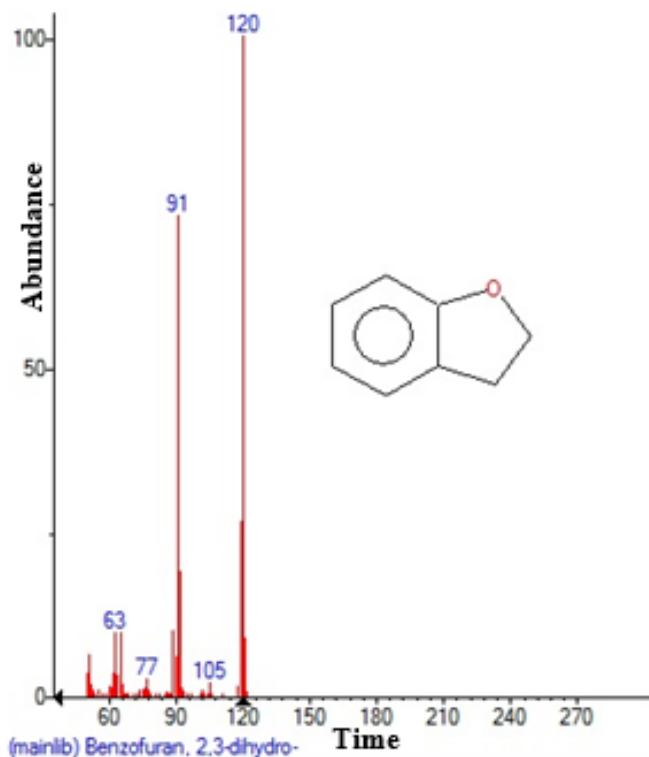


Figure 12. Structure of Benzofuran ,2,3-dihydro with 6.715 (RT) present in *Euphorbia lathyris*.

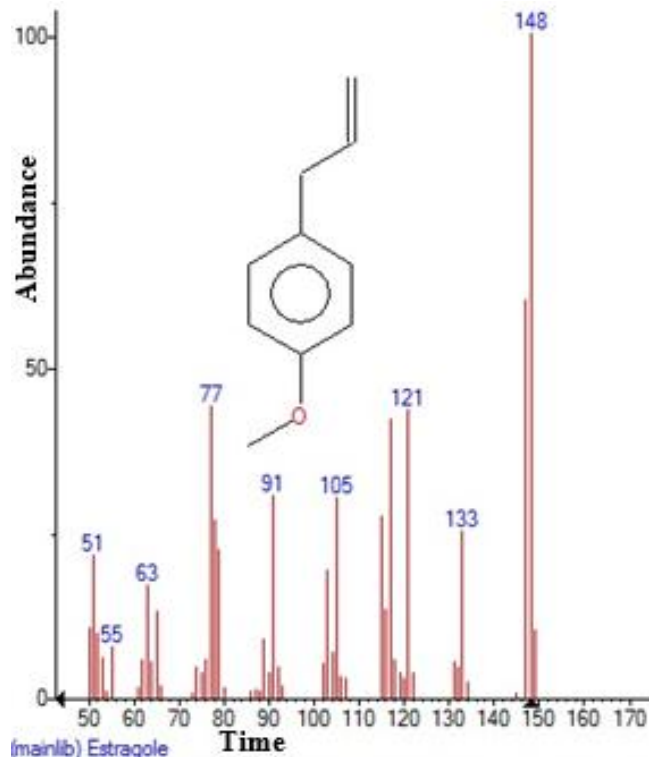


Figure 14. Structure of Estragole with 7.481 (RT) present in *Euphorbia lathyris*.

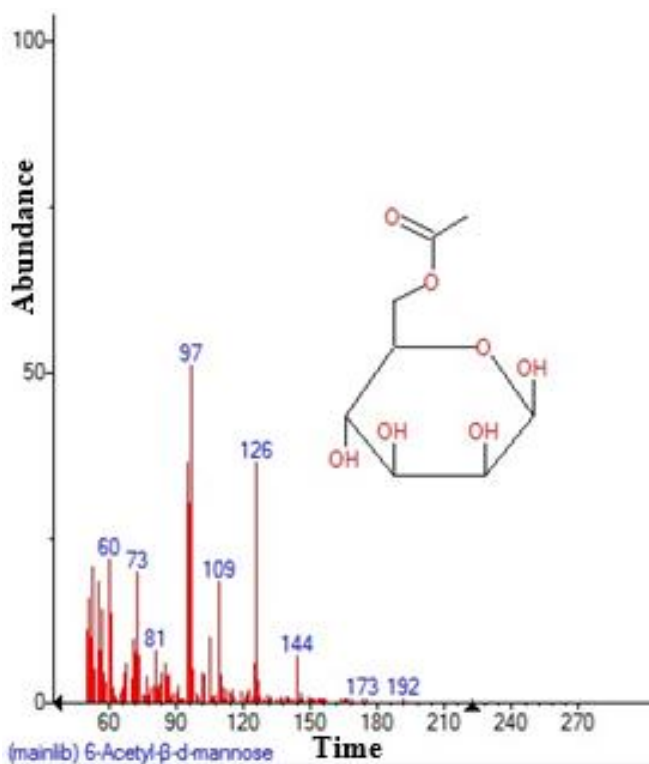


Figure 13. Structure of 6-Acetyl-β-d-mannose with 6.984 (RT) present in *Euphorbia lathyris*.

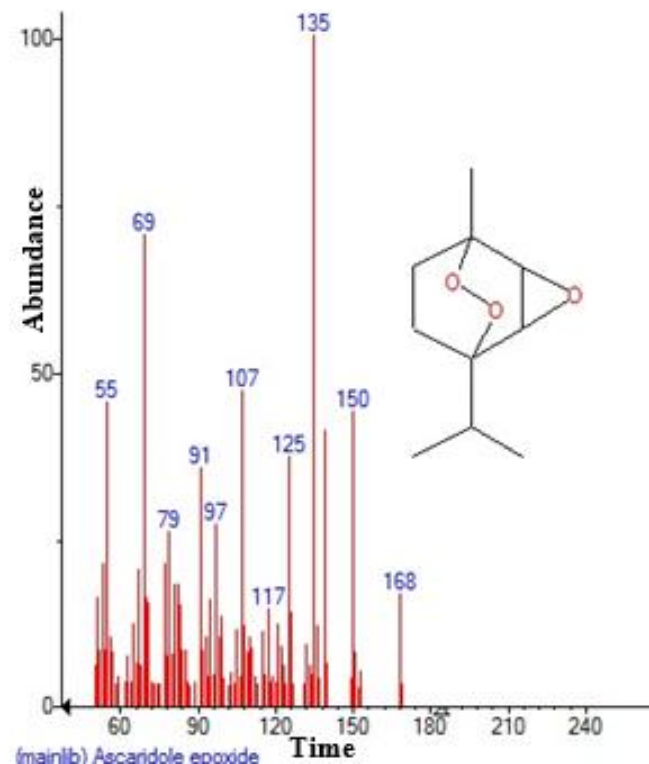


Figure 15. Structure of Ascaridole epoxide with 7.727 (RT) present in *Euphorbia lathyris*.

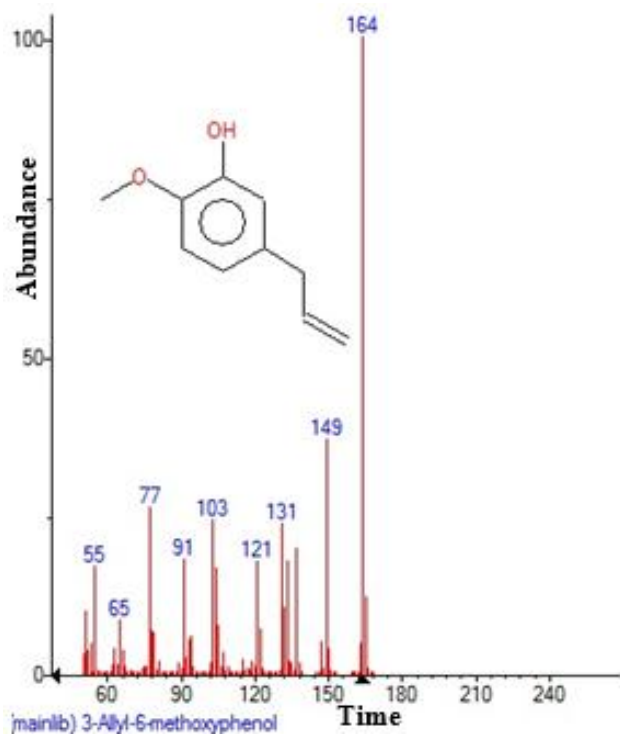


Figure 16. Structure of 3-Allyl-6-methoxyphenol with 8.443 (RT) present in *Euphorbia lathyris*.

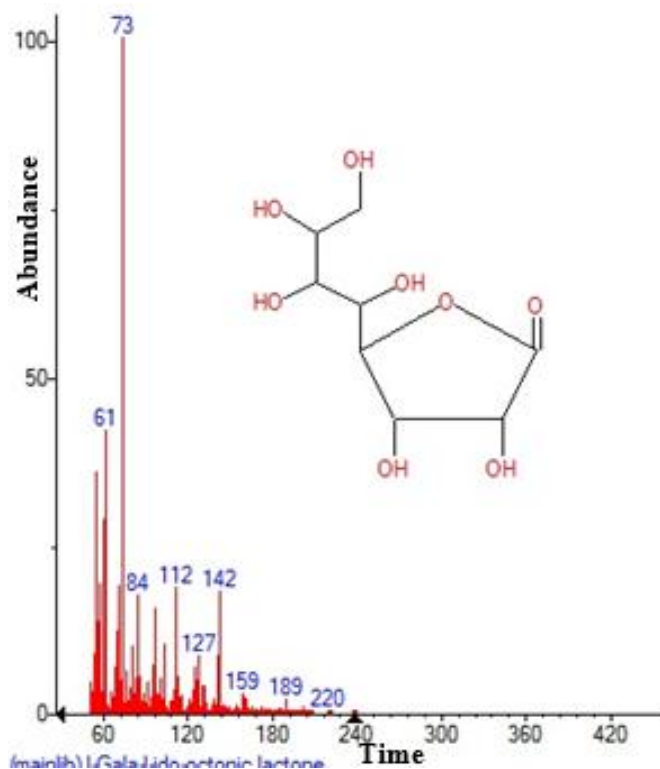


Figure 18. Structure of l-Gala-l-ido-octonic lactone with 10.743 (RT) present in *Euphorbia lathyris*.

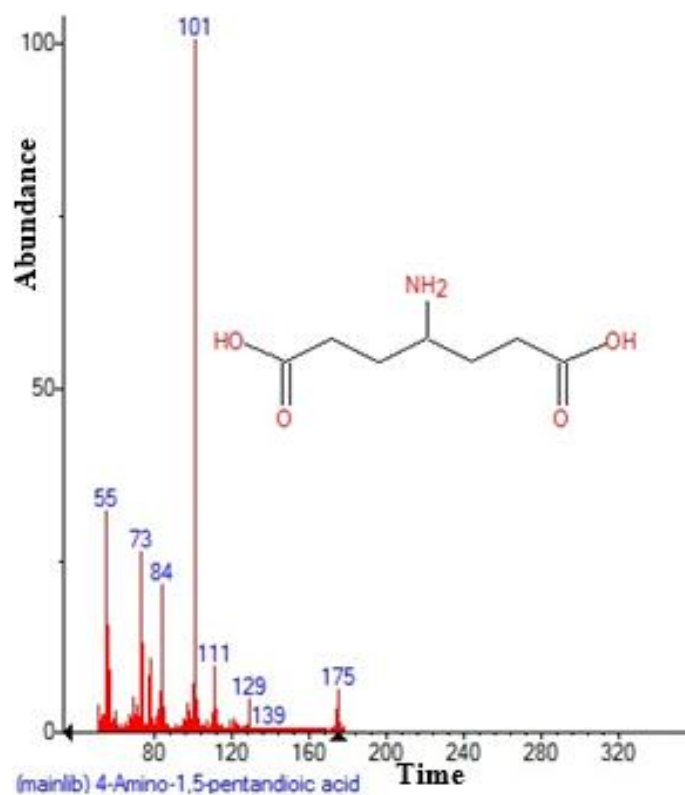


Figure 17. Structure of 4-Amino-1,5-pentandioic acid with 9.564 (RT) present in *Euphorbia lathyris*.

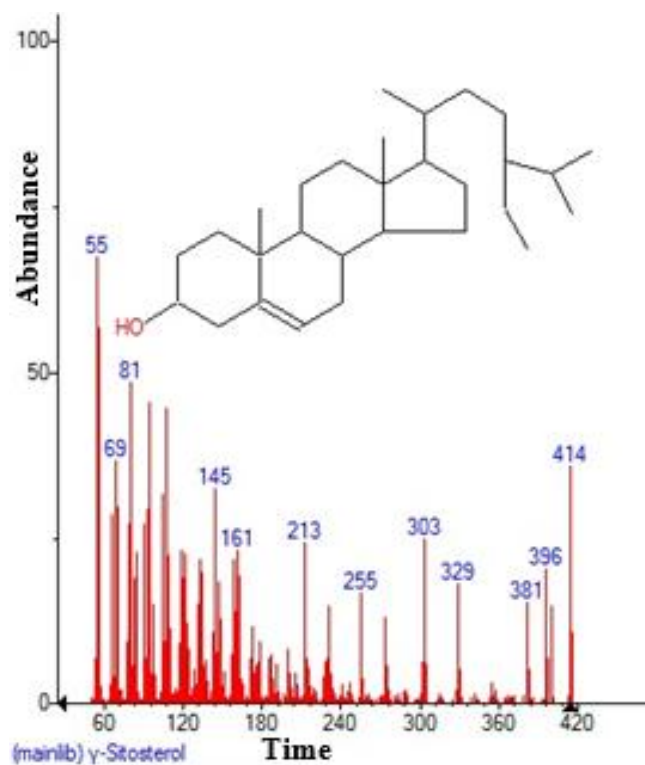


Figure 19. Structure of γ -Sitosterol with 15.023 (RT) present in *Euphorbia lathyris*.

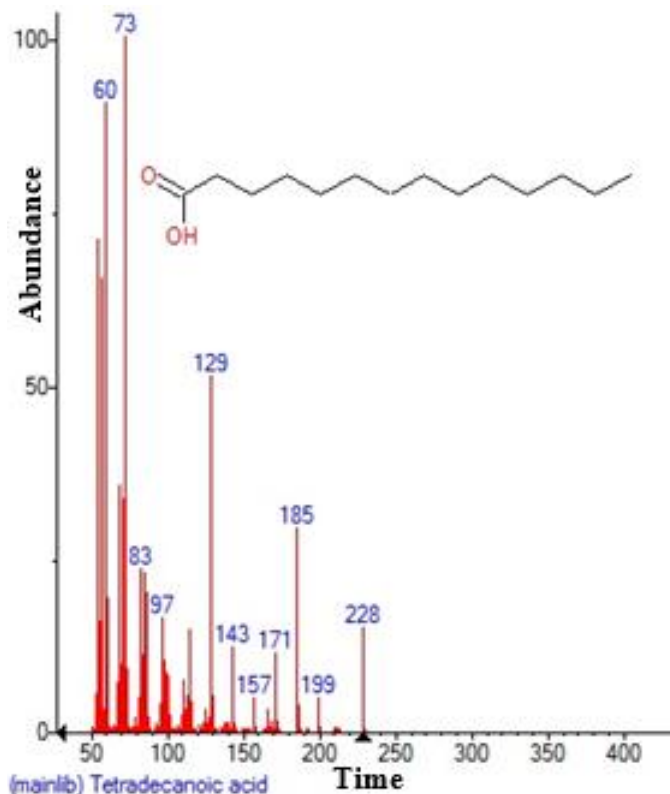


Figure 20. Structure of Tetradeconoic acid with 13.455 (RT) present in *Euphorbia lathyris*.

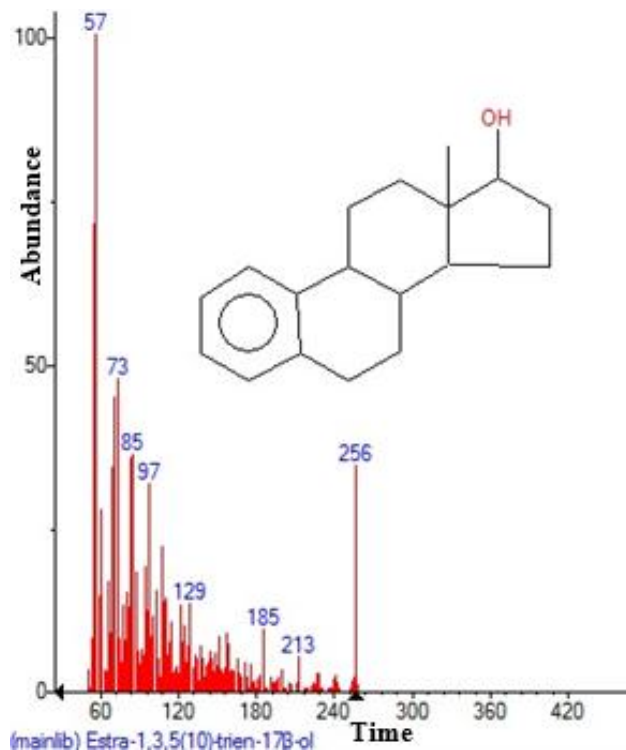


Figure 22. Structure of Estra -1,3,5(10)-trien-17β-ol with 16.007 (RT) present in *Euphorbia lathyris*.

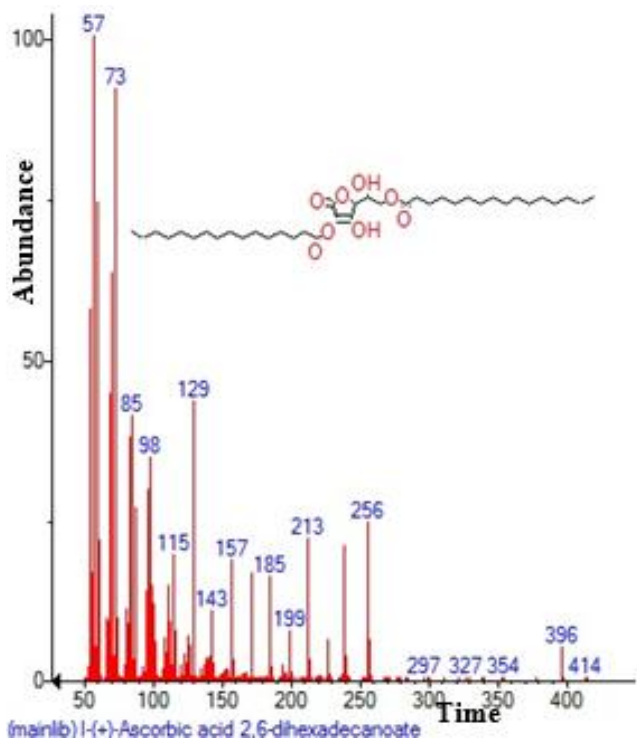


Figure 21. Structure of l-(+)-Ascorbic acid 2,6-dihexadecanoate with 15.486 (RT) present in *Euphorbia lathyris*.

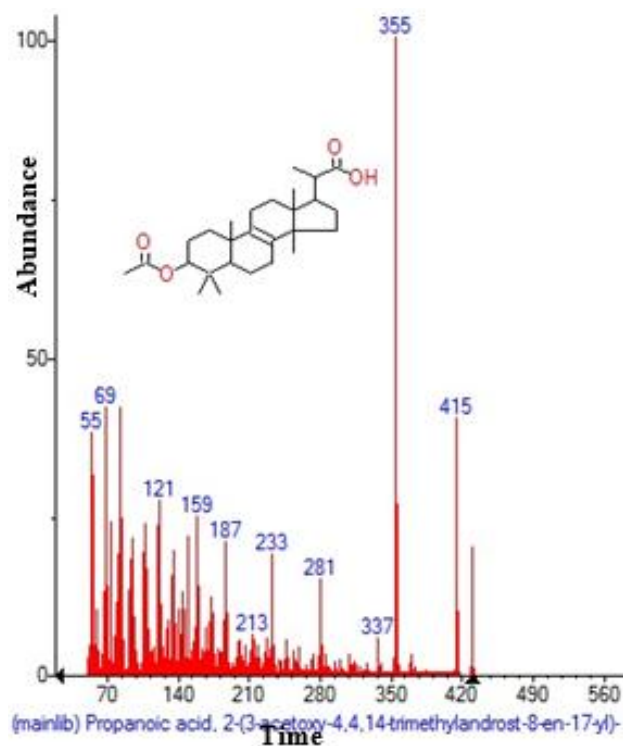


Figure 23. Structure of Propanoic acid ,2-(3-acetoxy-4,4,14-trimethylandro-8-en-17-yl) with 16.745 (RT) present in *Euphorbia lathyris*.

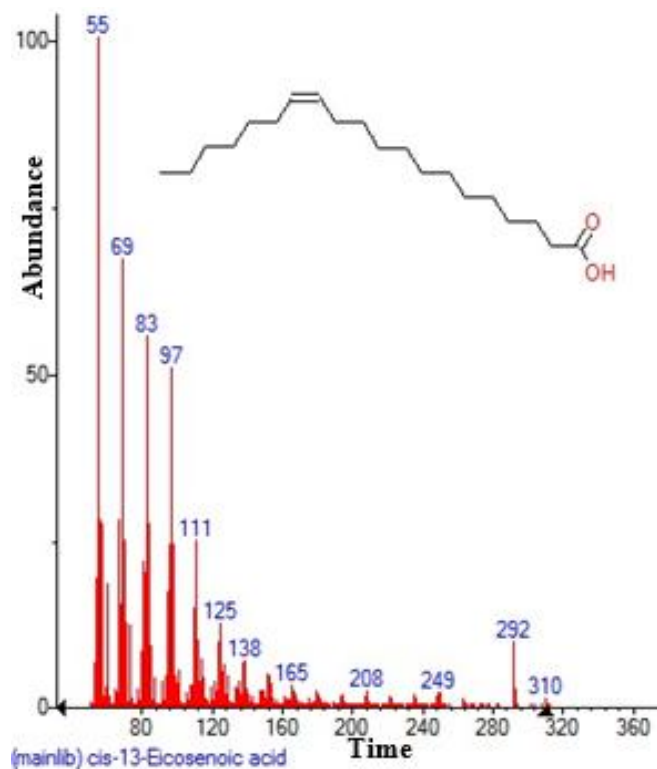


Figure 24. Structure of Cis-13-Eicosenoic acid with 18.914 (RT) present in *Euphorbia lathyris*.

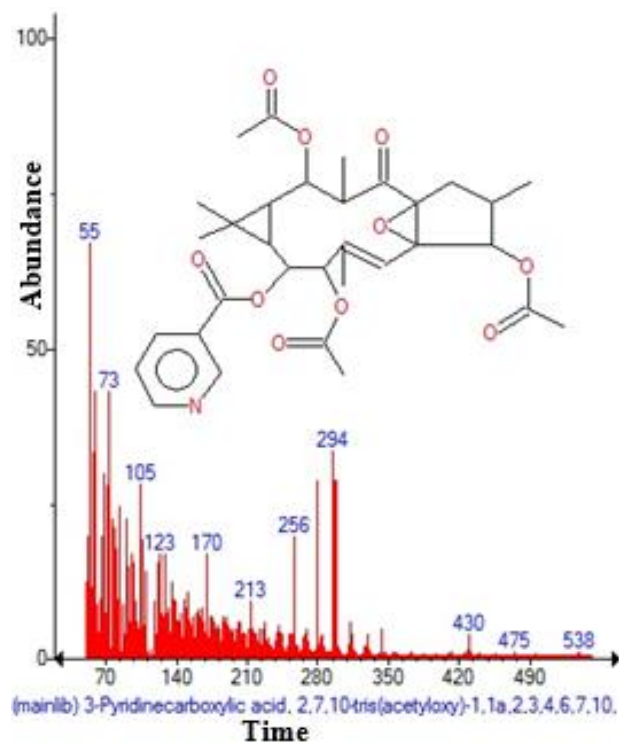


Figure 26. Structure of 3-Pyridinecarboxylic acid, 2,7,10-tris(acetyloxy)-1,1a,2,3,4,6,7,10 with 19.246 (RT) present in *Euphorbia lathyris*.

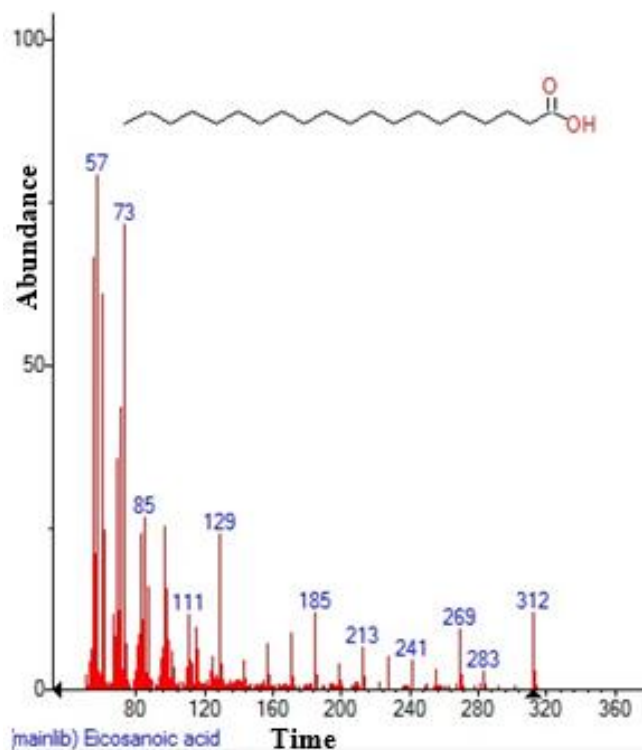


Figure 25. Structure of Eicosanoic acid with 19.051 (RT) present in *Euphorbia lathyris*.

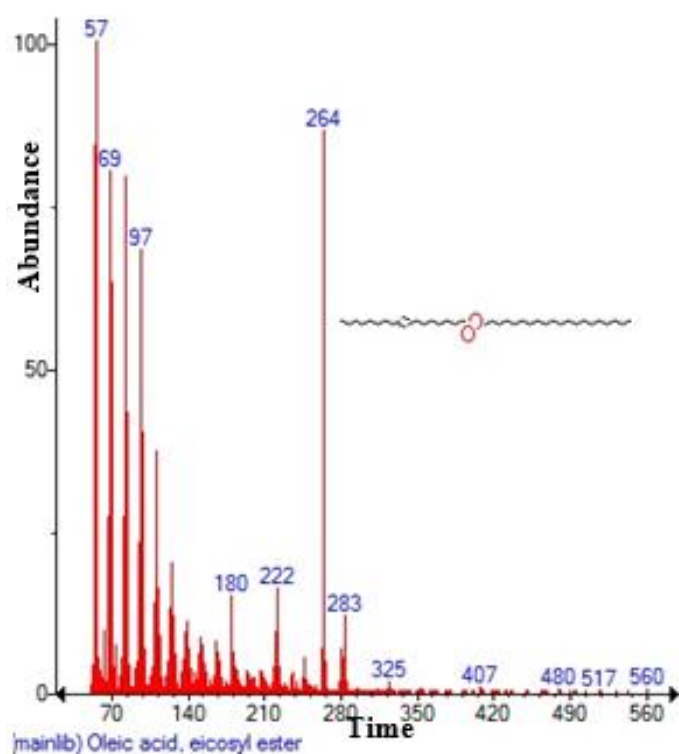


Figure 27. Structure of Oleic acid, eicosyl ester with 20.339 (RT) present in *Euphorbia lathyris*.

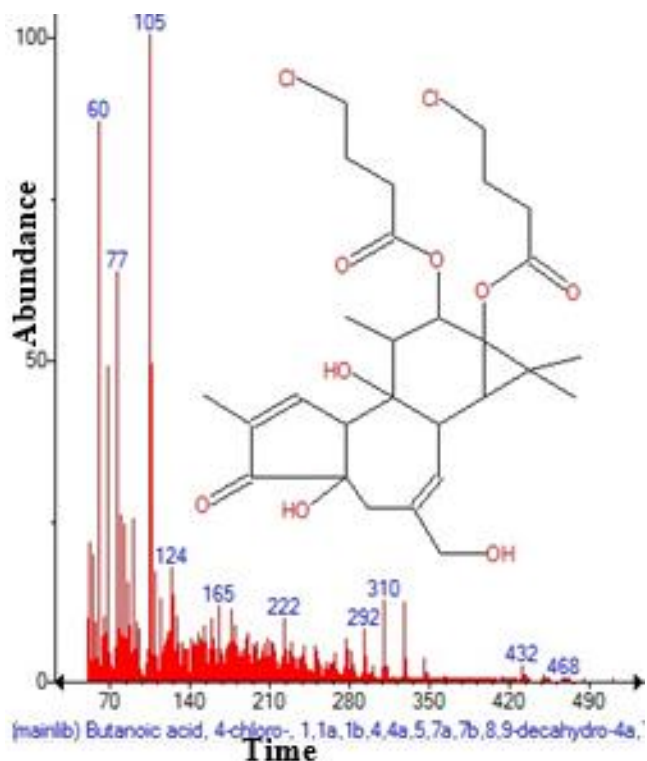


Figure 28. Structure of Butanoic acid , 4-chloro- ,1,1a,1b,4,4a,5,7a,7b,8,9-decahydro-4a with 21.083 (RT) present in *Euphorbia lathyris*.

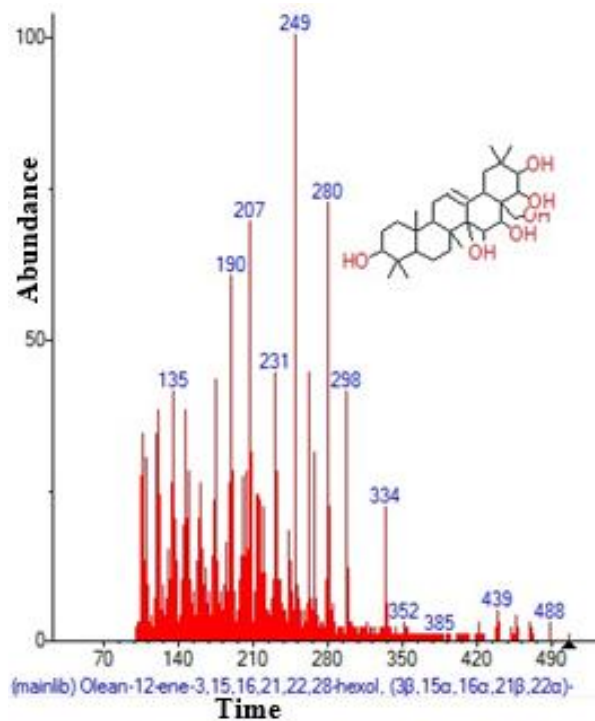


Figure 30. Structure of Olean -12-ene-3,15,16,21,22,28-hexol, (3β,15α,16α,21β,22α) with 21.603 (RT) present in *Euphorbia lathyris*.

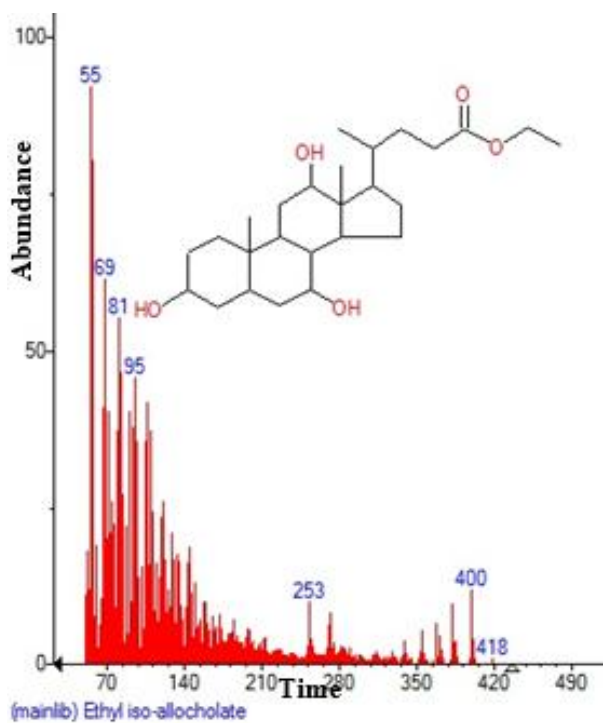


Figure 29. Structure of Ethyl iso –allocholate with 21.134 (RT) present in *Euphorbia lathyris*.

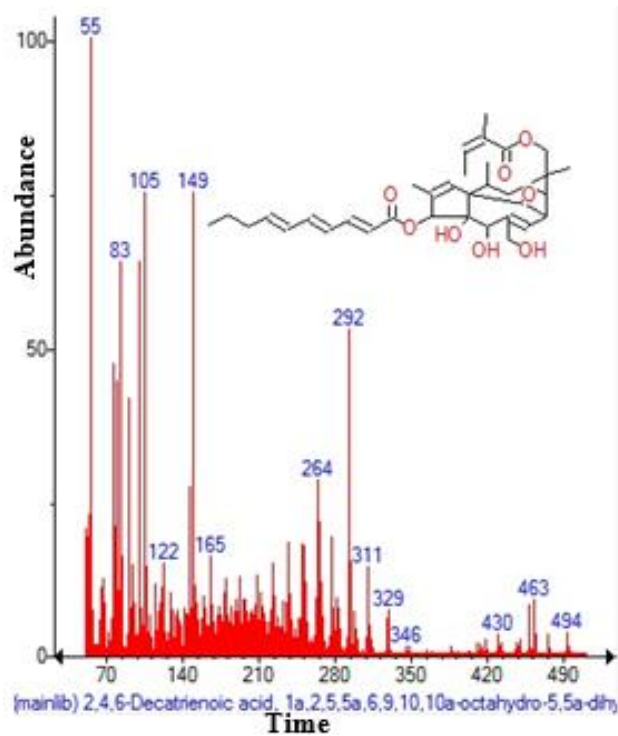


Figure 31. Structure of 2,4,6-Decatrienoic acid ,1a,2,5,5a,6,9,10,10a-octahydro-5,5a-dihy with 21.878 (RT) present in *Euphorbia lathyris*.

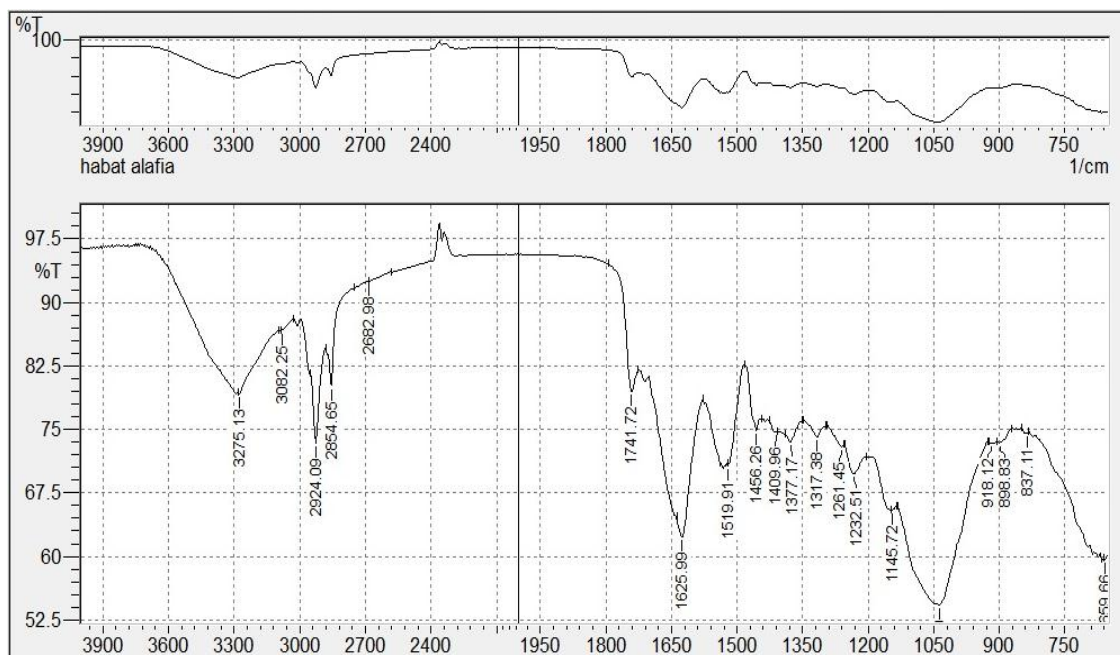


Figure 32. FT-IR profile of *Euphorbia lathyris*.

Conclusion

E. lathyris is native plant of Iraq. It contains chemical constitutions which may be useful for various herbal formulation as anti-inflammatory, analgesic, antipyretic, cardiac tonic, and antiasthmatic.

Conflict of interest

The authors have not declared any conflict of interest

ACKNOWLEDGEMENTS

The authors would like to express their gratitude to Dr. Abdul-ghafar for his valuable suggestions and comments. They also which to express their deepest gratitude to Prof. Dr. Adul-Kareem for his valuable contributions and support throughout the study.

REFERENCES

- Al-Marzoqi AH, Hadi MY, Hameed IH (2016). Determination of metabolites products by *Cassia angustifolia* and evaluate antimicrobial activity. *J. Pharmacogn. Phytother.* 8(2):25-48.
- Al-Marzoqi AH, Hameed IH, Idan SA (2015). Analysis of bioactive chemical components of two medicinal plants (*Coriandrum sativum* and *Melia azedarach*) leaves using gas chromatography-mass spectrometry (GC-MS). *Afr. J. Biotechnol.* 14(40):2812-2830.
- Altameme H J, Hadi MY, Hameed IH (2015a). Phytochemical analysis of *Urtica dioica* leaves by fourier-transform infrared spectroscopy and gas chromatography-mass spectrometry. *J. Pharmacogn. Phytother.* 7(10):238-252.
- Altameme HJ, Hameed IH, Abu-Serag NA (2015b). analysis of bioactive phytochemical compounds of two medicinal plants, *Equisetum arvense* and *Alchemilla vulgaris* seed using gas chromatography-mass spectrometry and fourier-transform infrared spectroscopy. *Malays. Appl. Biol.* 44(4):47-58.
- Altameme HJ, Hameed IH, Idan SA, Hadi MY (2015c). Biochemical analysis of *Origanum vulgare* seeds by fourier-transform infrared (FT-IR) spectroscopy and gas chromatography-mass spectrometry (GC-MS). *J. Pharmacogn. Phytother.* 7(9):221-237.
- Buenz EJ, Schnepfle DJ, Bauer BA, Elkin PL, Riddle JM, Motley TJ (2004). Techniques: bioprospecting historical herbal texts by hunting for new leads in old tomes. *Trends Pharmacol. Sci.* 25:494-498.
- Cai YZ, Luo Q, Sun M, Corke H (2004). Antioxidant activity and phenolic compounds of 112 Chinese medicinal plants associated with anticancer. *Life Sci.* 74:2157-2184.
- Corro G, Bañuelos F, Vidal E, Cebada S (2014). Measurements of Surface Acidity of Solid Catalysts for Free Fatty Acids Esterification in *Jatropha curcas* crude oil for biodiesel production. *Fuel.* 115:625-628.
- Hadi MY, Mohammed GJ, Hameed IH (2016). Analysis of bioactive chemical compounds of *Nigella sativa* using gas chromatography-mass spectrometry. *J. Pharmacogn. Phytother.* 8(2):8-24.
- Hameed IH, Abdulzahra AI, Jebor MA, Kqueen CY, Ommer AJ (2015a). Haplotypes and variable position detection in the mitochondrial DNA coding region encompassing nucleotide positions. *Mitochondrial DNA.* 26(4):544-9.
- Hameed IH, Hamza LF, Kamal SA (2015b). Analysis of bioactive chemical compounds of *Aspergillus niger* by using gas chromatography-mass spectrometry and fourier-transform infrared spectroscopy. *J. Pharmacogn. Phytother.* 7(8):132-163.
- Hameed IH, Hussein HJ, Kareem MA, Hamad NS (2015c). Identification of five newly described bioactive chemical compounds in methanolic extract of *Mentha viridis* by using gas chromatography-mass spectrometry (GC-MS). *J. Pharmacogn. Phytother.* 7(7):107-125.
- Hameed IH, Ibraheem IA, Kadhim HJ (2015d). Gas chromatography mass spectrum and fourier-transform infrared spectroscopy analysis of methanolic extract of *Rosmarinus officinalis* leaves. *J. Pharmacogn. Phytother.* 7(6):90-106.
- Hamza LF, Kamal SA, Hameed IH (2015). Determination of metabolites products by *Penicillium expansum* and evaluating antimicrobial activity. *J. Pharmacogn. Phytother.* 7(9):194-220.

- Hussein AO, Mohammed GJ, Hadi MY, Hameed IH (2016a). Phytochemical screening of methanolic dried galls extract of *Quercus infectoria* using gas chromatography-mass spectrometry (GC-MS) and Fourier transform-infrared (FT-IR). J. Pharmacogn. Phytother. 8(3):49-59.
- Hussein HJ, Hadi MY, Hameed IH (2016b). Study of chemical composition of *Foeniculum vulgare* using Fourier transform infrared spectrophotometer and gas chromatography - mass spectrometry. J. Pharmacogn. Phytother. 8(3):60-89.
- Hussein HM, Hameed IH, Ibraheem OA (2016c). Antimicrobial activity and spectral chemical analysis of methanolic leaves extract of *Adiantum capillus-veneris* using GC-MS and FT-IR spectroscopy. Int. J. Pharmacogn. Phytochem. Res. 8(3).
- Jasim H, Hussein AO, Hameed IH, Kareem MA (2015). Characterization of alkaloid constitution and evaluation of antimicrobial activity of *Solanum nigrum* using gas chromatography mass spectrometry (GC-MS). J. Pharmacogn. Phytother. 7(4):56-72.
- Liu H, Hong LZ, Wang MW (2011). Progress of Study on Energy Plant *Euphorbia lathyris* L. Anhui Agric. Sci. Bull. 17:119-120.
- Park EJ, Pezzutto JM (2002). Botanicals in cancer chemoprevention. Cancer Metastasis Rev. 21:231-255.
- Reddy VBM, Reddy K, Gunasekar D, Murthy M, Caux C, Bodo B (2003). A new sesquiterpene lactone from *Bombax malabaricum*. Chem. Pharm. Bull. 51:458-459.
- Shahat AA, Hassan RA, Nazif NM, Van MS, Pieters L, Hammuda FM (2003). Isolation of mangiferin from *Bombax malabaricum* and structure revision of shamimin. Planta Med. 69:1068-1070.
- Tapiero H, Tew KD, Ba N, Mathe G (2002). Polyphenols: do they play a role in the prevention of human pathologies? Biomed. Pharmacother. 56:200-207.
- Wei WL, Jin MY, Ma C (2007) Fatty Acid Composition Analysis of *Euphorbia lathyris* L. Seed Oil. China Oils Fats 32:70-71.



Journal of Pharmacognosy and Phytotherapy

Related Journals Published by Academic Journals

- *African Journal of Pharmacy and Pharmacology*
- *Research in Pharmaceutical Biotechnology*
- *Medical Practice and Reviews*
- *Journal of Clinical Pathology and Forensic Medicine*
- *Journal of Medicinal Plant Research*
- *Journal of Drug Discovery and Development*
- *Journal of Clinical Virology Research*

academicJournals